NANOscientific
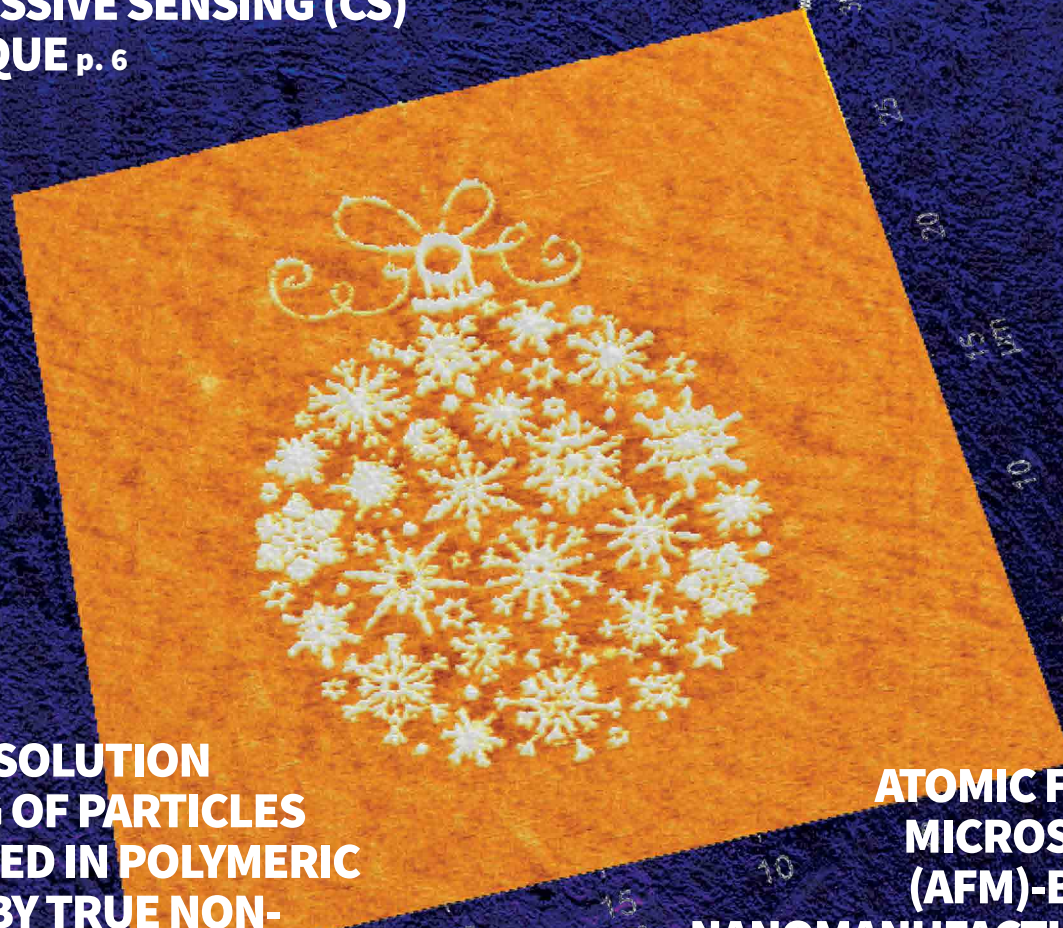
The Magazine for NanoScience and Technology

MOLECULAR VIBRATIONAL BASED SURFACE SENSITIVE IMAGING – SUM FREQUENCY GENERATION (SFG) MICROSCOPY WITH COMPRESSIVE SENSING (CS) TECHNIQUE p. 6

THE DEVELOPMENT OF SCANNING ELECTROCHEMICAL CELL MICROSCOPY (SECCM) p. 11

HIGH RESOLUTION IMAGING OF PARTICLES DISPERSED IN POLYMERIC MATRIX BY TRUE NON-CONTACT™ MODE ATOMIC FORCE MICROSCOPY p. 13

ATOMIC FORCE MICROSCOPE (AFM)-BASED NANOMANUFACTURING ASSISTED BY VIBRATION AND HEAT p. 18

NANOSCALE MATERIAL PATTERNING USING ATOMIC FORCE MICROSCOPY NANO-LITHOGRAPHY p. 21

BULK PHOTOVOLTAIC EFFECT IN FERROELECTRIC MATERIALS p. 24

TABLE OF CONTENTS

NanoScientific Vol 18 Winter 2020

p. 6

p. 11

p. 18

Line Profile

p. 21

INSET PHOTO ON COVER:

The AFM topography image reveals that the design of the nanoscale oxide patterns generated by voltage-biased AFM nanolithography using Park NX10 is a Christmas ball pattern with a diameter of approximately 17 µm and composed of multiple tiny structures with heights ranging from 0.2–1.5 nm.
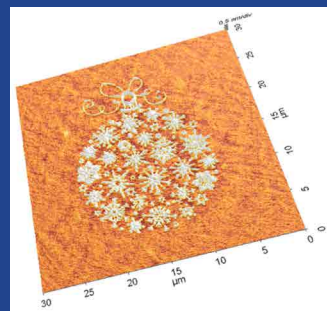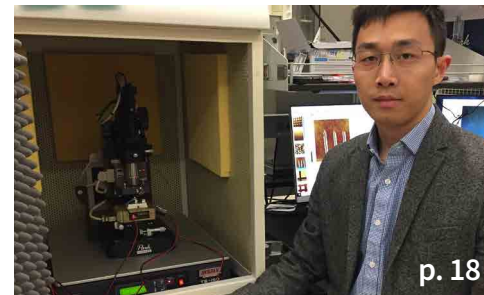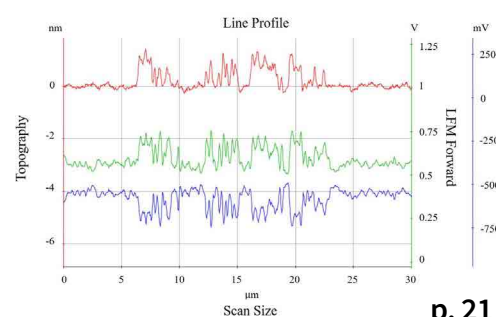
MESSAGE FROM EDITOR

Welcome to our first issue of NanoScientific in 2020!

We are very excited to publish articles highlighting applications that showcase many of the advancements made in Nanometrology in the past year.

We welcome our Editorial Board for another year and are also happy to announce after sponsoring with Park Systems, six very successful NanoScientific Symposiums in 2019, we will sponsor NanoScientific Symposiums again in 2020 at locations across the globe.

Below is a New Years Greeting from our publisher who we thank for allowing this publication to grow and flourish.

We wish all of you a very Happy New Year!

Keibock Lee
Editor-in-Chief

Greetings,
As we approach the end of another exciting year, I would like to send my appreciation to all our customers, employees and stakeholders for helping make 2019 an exceptional year for Park Systems.

Although the national economy continued to stagnate, our company continued to demonstrate steady growth over the past year and surpassed 50 billion KRW in annual sales, reflecting our best year ever. Contributing to this milestone, major semiconductor manufacturers around the world are expanding the scope of application of AFM (atomic force microscopy) as they move to mass production processes.

In addition, the future landscape for Park Systems is very bright, as manufacturers are requiring AFM systems not only in the front-end-of-line but also in the back-end-of-line, photomask and display process. As our continued expansion requires increasing workloads, we are constantly recruiting talented workers both at home and abroad to provide the hallmark exceptional service that our reputation is built upon. We are also excited that Park Systems headquarters has experienced an expansion, as well, to the 15th floor of the Korea Advanced Nano Fab Center.

NanoScientific Symposiums, which are sponsored and executed worldwide by Park Systems has also expanded in 2019, with events held in China (Tianjin U), Korea (Suwon Convention Center), Europe (U Bologna), Southeast Asia (NUS), Mexico (UNAM), and the United States (SUNY Albany), showcasing presenters who are leaders in the field of SPM, nanometrology and more.

Park Systems won several premier awards in 2019, including the Prime Minister's Award at the Nano Korea 2019 and the Deputy Prime Minister's Award at the 2019 Happy MSE Management Grand Prize, and was also selected as the 'KOSDAQ Rising Star' for two consecutive years by the Korea Exchange. Park is very proud to be selected as an excellent organization for human resource development business (Gyeonggi-do Institute of Economic Science).

Looking back over 2019, I would like to express my sincere gratitude to all of you who have helped us achieve all of this tremendous success. We promise to continue to work hard to make 2020 another stellar year.

Wishing each of you a safe and prosperous New Year,

Dr. Sang-il Park
Founder and CEO Park Systems

MOLECULAR VIBRATIONAL BASED SURFACE SENSITIVE IMAGING

SUM FREQUENCY GENERATION (SFG) MICROSCOPY WITH COMPRESSIVE SENSING (CS) TECHNIQUE

Hao Li and Steven Baldelli
Department of Chemistry
University of Houston
Houston, TX 77204-5003

HAO LI received his bachelor's degree in chemistry at Nanjing University in 2015. While there, he studied surface enhanced infrared spectroscopy with Prof. Xinghua Xia.

From 2015, Hao Li joined Dr. Steven Baldelli's group. His research topic is to study CO-Pt electrode interface using compressive sensing sum frequency generation microscopy combined with electrochemistry.

STEVEN BALDELLI is a professor of chemistry at the University of Houston. He received his BS in chemistry at Framingham State College in Framingham, Massachusetts and Ph.D. in chemistry from Tufts University with Mary Shultz.

His postdoctoral work was at the University of California, Berkeley with Gabor Somorjai and Phil Ross. Since at the University of Houston, his research has focused on; surface chemistry of ionic liquids, corrosion an inhibition of metals, electrocatalysis, surface adsorption, electrochemistry, and nonlinear optical microscopy.

Introduction

SFG is a second order nonlinear optical process. Compared with other vibrational spectroscopy techniques such as Infrared and Raman, SFG are widely applied to study interface systems due to its high surface selectivity. This property makes it useful into microscopy applications to map the molecular vibrational contrast of the interfaces. From the process first observed in 1980s[1, 2], SFG is developed to study complex interface systems such as monolayer on metal surfaces[3-6] and biomaterials system[7]. However, the low signal intensity and long acquisition time are two main limitations for good imaging results.

To reduce the data acquisition time, the sampling process of SFG microscopy is combined with Compressive Sensing (CS) technique, which requires fewer samples or measurements than Nyquist–Shannon sampling theorem[8-10]. Meanwhile, the CS microscopy technique maintains higher intensity of each single measurement compared to scanning microscopy techniques because each measurement samples half of the image. Therefore it results in a high imaging speed with good image quality. With the CS technique, the broadband spectroscopic SFG system is able to apply on studying the complex molecular mixture on the interface.

SFG Spectroscopy

SFG is a surface sensitive technique that provides information about the vibrational modes of molecules at the interface. SFG process occurs when two pulsed laser beams, an infrared (IR) and a visible, spatially and temporally overlap at an interface[11] as shown in figure 1. Their interaction with the material produces an SF beam, whose frequency equals the sum of the two incident frequencies, i.e.,.

$$\omega_{SF} = \omega_{IR} + \omega_{vis}.$$
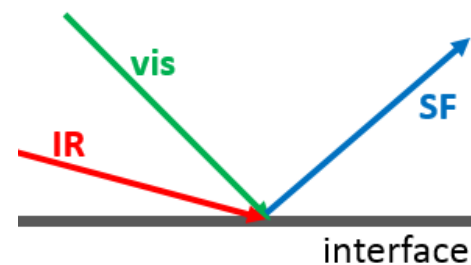
Figure 1 - SFG beam diagram

The relationship between the intensity of the SF beam and the electric fields of the two incident beams is given by:

$$I_{SF} \propto |\chi^{(2)} : E_{IR} \, E_{vis}|^2$$

Where $\chi^{(2)}$ is the second-order nonlinear susceptibility[12]. As a third rank tensor, the value of $\chi^{(2)}$ equals zero for centrosymmetric systems[2]. As a result, SFG process only occurs at interface, which breaks the centrosymmetric compare to bulk volume.

CS-SFG microscopy

Figure 2 - SFG microscope setup

In figure 3, CS-SFG microscopy setup, one visible beam (green line, 513 nm) irradiates at 45 degrees while one broadband IR beam (red line) irradiates at 75 degrees[13, 14]. After reaching spatial and temporal overlap on sample surface, the generated SF beam (blue line) is split by the spectrometer and detected by the CCD array.
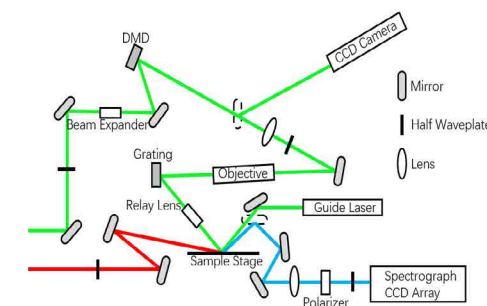
Figure 3 - Scheme of SFG microscope optics diagram

Figure 4 - CS-SFG imaging process

The digital mirror device (DMD) is applied to form a random 2D pattern structural visible beam.

The imaging reconstruction process shown in figure 4 is based on the spectroscopic information obtained from CCD array related to the structural visible beam from each DMD pattern. Compared to single wavenumber camera detector, the CS technique has the advantage to apply broadband system to acquire more complete molecular information, for example the entire C-H vibrational modes range, with increasing efficiency of imaging.

Compressing Ratio Influence on Image Quality

The CS technique is based on the fact that significant signals in nature are sparse. Therefore, the majority of information of the images comes from a small part of the signal with large coefficients. Measuring only the signals with high coefficients, compressed sampling is achieved. That is, less measurements compare to usual imaging process is capable of revealing most of the information in the images.

A striping self-assemble monolayer (SAM) sample was tested to examine the effect of the compressing ratio to the image quality[15].3 mM 1-octadecanethiol (ODT) ethanol solution was stamped on the gold evaporated silicon wafer by a homemade striping PDMS stamp. The exposed gold surface was then etched to form ODT SAM on gold stripes sample. The sample was tested with the IR beam focused at 2880 cm^{-1}.

The figure 5 shows the reconstruction SFG images with various number, 20%, 40%, 60%, 80% and 100%, of the total 1024 DMD patterns, which is the total number of patterns available to 32 × 32 pixels. From the result, the stripes pattern become clearer with the increasing number of patterns. And with 40% of the available patterns, the image is clear enough to provide the stripes information. Therefore, by keeping most of the information for a clear enough image, imaging process can be compressed. Based on this advantage, shorter acquisition time is needed for each imaging process, which makes it possible to monitor the surface condition changes in a small time scale. As to application, the SFG microscopy can be used to monitor the kinetics of the surface reactions, such as the wetting process of liquid on solid surface, which finishes in a relative short time.

Structural Hyperspectral Imaging of Self-Assembled Monolayers (SAMS)

SFG microscopy is a hyperspectral imaging process that reveals not only the surface morphology, but also the chemical information within surface area. This feature makes SFG useful in studying the spatial-chemical distribution on the surface. Microcontact printing is an often used technique to form patterns of SAMS on substrate whose domains follows the PDMS stamp structure. Alkanethiol molecules are widely studied in surface chemistry. Studying how the SAMS of alkanethiol molecules distribute and
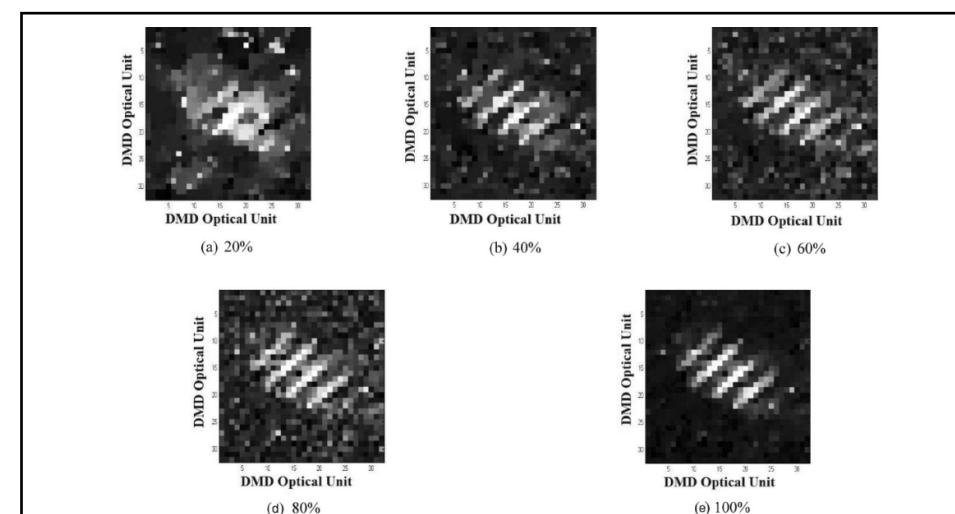
Figure 5 Effect of number of patterns on SFG imaging quality[15]
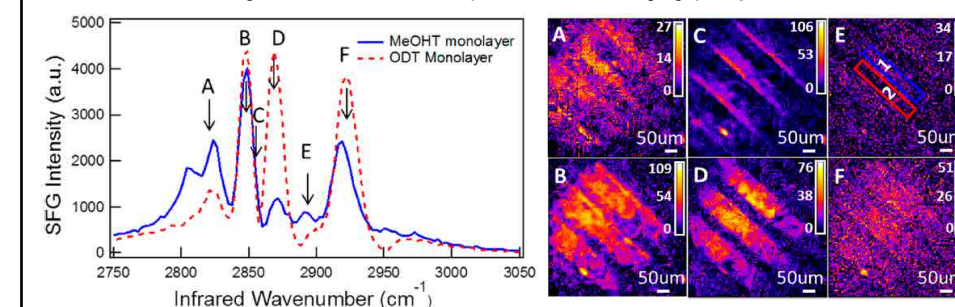
Figure 6 - SFG spectra of ODT and MeOHT[14]. Figure 7 - SFG images of ODT and MeOHTstripe pattern mixture[14]

influence the surface property can be interesting especially in some metal corrosion problems[16]. In SFG microscopy, the alkanethiol molecules distribution is studied by focusing the IR at C-H vibrational range. 1-octadecanethiol (ODT) and 16-methoxy-1-hexadecanethiol (MeOHT) mixture are studied here with stripe patterns[14]. Figure 6 shows the SFG spectra of pure molecules. By setting the IR wavenumber to match the vibrational modes, these two molecules can be distinguished due to the difference in their spectra.

From the SFG spectra of the two molecules, ODT has higher intensity at peak position B, D and F while MeOHT is higher at peak A and E. The reconstruction SFG images shown as figure 7 match the spectra result that when IR wavenumber is set at B, D and F peak wavenumber positions, the brighter stripes are located at region 1 shown in image E while image A and C have brighter stripes in region 2. The comparison between the SFG spectra from region 1 and 2 with the pure chemicals in figure 8 shows that MeOHT and ODT are located within these two stripe areas separately. The result proved that SFG microscopy can be used as a reliable imaging technique to observe not only the surface morphology but also the chemical information distribution.

Figure 9 Scheme of possible molecules adsorption modes[20]

Table 1 Peak comparison between experimental and theoretical results[20]

vibrational modes	flat-on	tilt-on	edge-on	experiment
CH (soft): 2910 cm⁻¹	●	×	×	●
CH₂ (ss): 2850 cm⁻¹	×	●	●	●
CH₂ (as): 2918 cm⁻¹	×	●	×	×
CH₃ (ss): 2875 cm⁻¹	×	●	●	●
CH₃ (ss-FR): 2935 cm⁻¹	×	●	●	●
CH₃ (as, out-of-plane): 2954 cm⁻¹	●	●	×	●
CH₃ (as, in-plane): 2962 cm⁻¹	×	●	●	●

"● represents the peak that is observed for the corresponding modes; × represents the peaks that are not captured for the mode.

calculated by the ratio of peak intensity from different polarization combinations. Besides SAMS, SFG can be applied to study more complex system such as the wetting process. The natural spreading process of long-chain alkanes on metal interface is widely studied because of its potential applications such as lubrication[17,18] or corrosion protection[19]. Dip-coating is a reliable method to simulate the natural wetting process at solid-liquid or solid-air interface.

Dotriacontane (DTC, n-C₃₂H₆₆) molecule films on polycrystalline gold surface system is studied[20]. Compared with SAMS system, part of the surface from dip-coating process is covered in homogeneously with either incomplete layers or multilayers. Combined with SFG microscopy technique, those in homogeneous distributions can be revealed from the domain structure in SFG images.

Figure 8 Comparison of SFG spectra from region 1 and 2 with pure ODT and MeOHT[14]

Surface Adsorbed Molecules Orientation Study

As a three photon nonlinear optical process, the different polarizations combination of the three beams is applied to study the orientations of the surface adsorbed molecules. SSP polarization, for example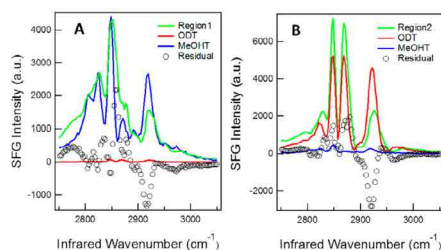, represents for S-, S-, and P- polarized output SF beam, input visible beam and input IR beam. From the C-H peaks assignment of the SFG spectrum, the geometry of methyl or methylene group can be determined. The tilt angle of the alkane chain can be
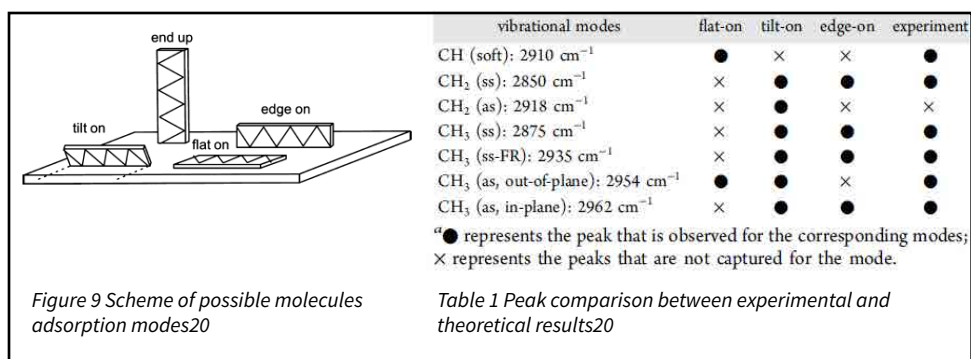
More details about the molecules orientation can be determined by locating the SFG spectra information into the functional group of the molecule. If the all-transalkyl chain is not parallel to the surface, the local centrosymmetry between the two adjacent -CH₂ vibrations results in no -CH₂ peaks assignment by the SFG selection rule. Therefore, any observed -CH₂ peak can be a proof of the broken of local centrosymmetry, that is, a gauche conformation of the alkyl chain. Based on this, SFG spectroscopy information can reveal the molecules adsorption modes, such as flat-on[21-24], tilt-on[25,26] or edge-on[27-31], compared with the theoretical peaks assignment[21-31]in table 1. In other words, by setting the IR wave number at the unique peak belongs to different modes, the highlight areas shown in SFG image represent the molecules with specific adsorption modes.
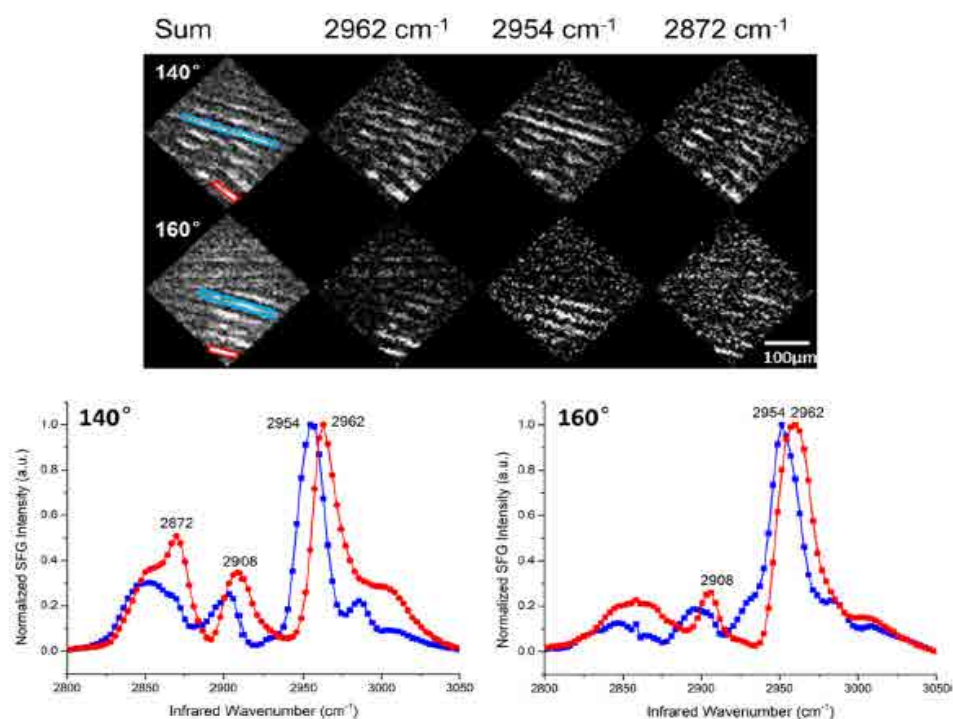

Figure 10 SFG images of different vibrational modes under different azimuthal angles. The spectra of the blue and red box areas were generated below[20]

Besides the adsorption modes, the orientation angle of the molecules within the same adsorption mode domain is another important property that can be studied by SFG microscopy. The SFG images were generated by summing over the wavenumber channels of entire C-H region to reveal the surface morphology in general. From the SFG image with the sum of C-H range vibrational modes in figure 10, the molecules are stripes structure after a dip-coating process. And the SFG spectra within one particular stripe suggest that the molecules not only belong to one adsorption mode but a combination.

To determine the molecular in-plane orientation of different adsorption modes within one stripe, the surface anisotropy diagram as figure 11is measured here by rotating the sample surface with different azimuthal angle. Basically, the geometry of the molecules with different adsorption modes belong to different symmetry point group, which has unique rotational representations. For example, flat-on mode molecules are C₂ conformation with a twofold rotation axis along z-direction while edge-on mode molecules are Cₛ symmetry with a symmetry mirror normal to x-y plane. By setting the IR wavenumber at 2908 cm⁻¹, the methylene group stretching mode as the unique peak for flat-on mode, the anisotropy diagram shows reasonable symmetry structure. By measuring the azimuthal angle value with maximum SFG intensity at 2908 cm⁻¹, the rotation axis of C₂ conformation can be determined, which represents for the orientation of the flat-on mode compare to the dip-coating direction. As a result, the details of how the DTC molecules adsorb on substrate, including the adsorption mode and the orientation, can be revealed from the SFG images.
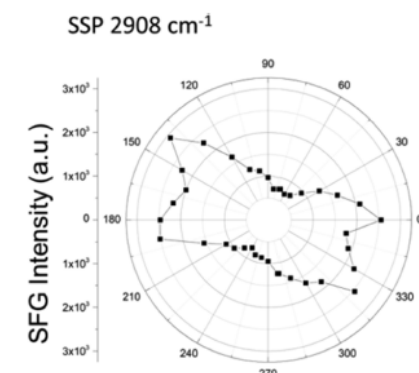
Figure 11 Polar plots of the intensity for methylene group stretching mode[20]

Aqueous System - Electrochemistry Study

Based on the features of CS-SFG microscopy mentioned above that we can observe the surface chemical domains and calculate the molecules behavior such as the orientations, it can be applied to more complex systems where other techniques are not available.

Another topic our group is focusing on is to test how the electrochemistry reactions happen on electrode surface in aqueous system. Most of the research focuses on using spectroscopy method to study the single crystal electrode surface, which signal only comes from the homogenous surface. However, for other natural polycrystalline electrodes, the spectroscopy cannot acquire the contribution from different crystal surfaces, especially some boundary or step conditions. SFG microscopy can be applied here to monitor the electrochemistry reactions process on different crystal surfaces and reveal the molecules' behaviors on boundary or step areas. Meanwhile, due to the surface selectivity, the thin electrolyte film within the beam path has no contribution to the SFG signal, which makes SFG not influenced by the bulk liquid phase. All of the features of SFG microscopy make it possible for an in-situ study of the molecules distribution on polycrystalline electrode surface.

CO-Pt electrode interface, as a widely studied system, was tested as an example for the SFG microscope. The hydrogen flame annealing treatment lets the Pt electrode surface form domain structures with clear boundaries shown in figure 12. By holding the potential of Pt at -0.15 V vs. Ag/AgCl in CO saturated 0.1 M H₂SO₄ electrolyte, CO gas molecules were adsorbed on Pt surface. The potential applied on Pt working electrode was then changed by potentiostat to examine the CO adsorption behaviors at different potentials. IR wavenumber was set near 2080 cm⁻¹ to measure the C-O stretching mode on top site of Pt. The wavenumber distribution was mapped with nonlinear fitting program though Mathematica as figure 13. From the mapping result, the wavenumber of the C-O stretching has a blue shift with an increasing potential following the stark shift effect. Meanwhile, part of the CO signal disappears at 0.50 V vs. Ag/AgCl, which indicates the CO

molecules adsorbed on the bottom two domains were oxidized and desorbed at higher potential. That is, SFG microscopy is able to show the difference of oxidation potential of CO on different surface domains, which cannot be revealed by average spectroscopy technique.
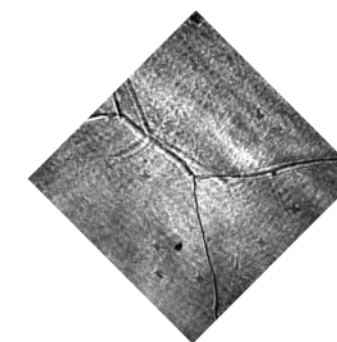
Figure 12 Optical image of polycrystalline Pt electrode surface

mapping as peak wavenumber (cm⁻¹)
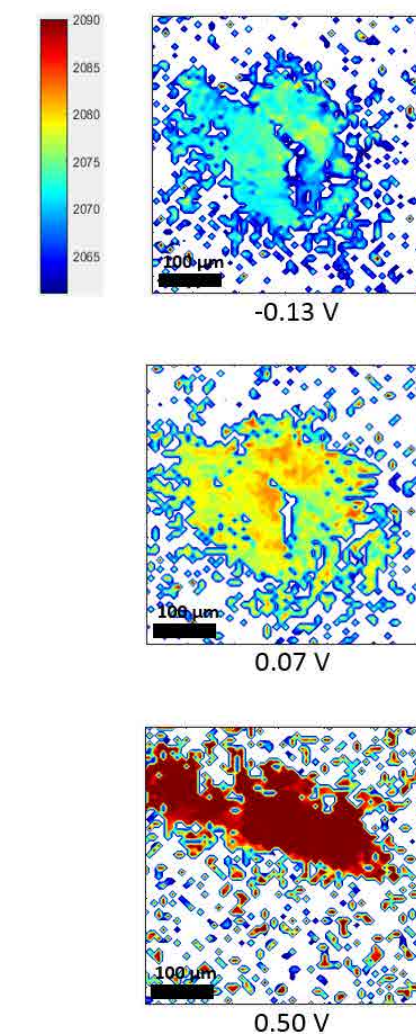
Figure 13 Fitting SFG wavenumber images of CO adsorption on Pt electrode at different potential vs. Ag/AgCl

Conclusion

SFG microscopy is a powerful technique for surface science due to its unique surface selectivity feature. It can be applied to distinguish the molecules distribution of the mixture on the surface. Based on SFG spectroscopy, the orientation and the adsorption mode can be measured. For more complicated system, for example the solid-liquid electrode surface, SFG microscopy has its advantages for in-situ study. Combined with CS technique, the imaging process of SFG microscopy can be compressed, which allows to capture the fast reaction process for solving dynamics problem.

Acknowledge

References

(1) Hunt, J. H.; Guyot-Sionnest, P.; Shen, Y. R. Observation of C-H Stretch Vibrations of Monolayers of Molecules Optical Sum Frequency Generation. Chem. Phys. Lett.1987, 133, 189−192.
(2) Zhu, X. D.; Suhr, H.; Shen, Y. R. Surface Vibrational Spectroscopy by Infrared-Visible Sum Frequency Generation. Phys. Rev. B: Condens. Matter Mater. Phys. 1987, 35, 3047−3050.
(3) Cimatu, K. A.; Baldelli, S. Chemical Microscopy of Surfaces by Sum Frequency Generation Imaging. J. Phys. Chem. C2009, 113 (38), 16575−16588.
(4) Cimatu, K.; Baldelli, S. Sum Frequency Generation Microscopy of Microcontact-Printed Mixed Self-Assembled Monolayers. J. Phys. Chem. B2006, 110 (4), 1807−1813.
(5) Fang, M.; Baldelli, S. Grain Structures and Boundaries on Microcrystalline Copper Covered with an Octadecanethiol Monolayer Revealed by Sum Frequency Generation Microscopy. J. Phys. Chem. Lett. 2015, 6 (8), 1454−1460.
(6) Fang, M.; Santos, G.; Chen, X.; Baldelli, S. Roles of Oxygen for Methanol Adsorption on Polycrystalline Copper Surface Revealed by Sum Frequency Generation Imaging Microscopy. Surf. Sci.2016, 648, 35−41.
(7) Raghunathan, V.; Han, Y.; Korth, O.; Ge, N.; Potma, E. O. Rapid Vibrational Imaging with Sum Frequency Generation Microscopy. Opt. Lett. 2011, 36 (19), 3891−3893.
(8) Candes, E.; Romberg, J. Sparsity and Incoherence in Compressive Sampling. Inverse Problems2007, 23 (3), 969−985.
(9) Romberg, J. Imaging via Compressive Sampling [Introduction to Compressive Sampling and Recovery via Convex Programming]. IEEE Signal Processing Magazine2008, 25 (2), 14−20.
(10) Baraniuk, R. G. Compressive Sensing. IEEE signal processing magazine2007, 24 (4).11810.1109/MSP.2007.4286571.
(11) Bain, C. D. Sum-Frequency Vibrational Spectroscopy of The Solid/Liquid Interface. J. Chem. Soc., Faraday Trans. 1995, 91 (9), 1281−1296.
(12) Shen, Y. Surface Properties Probed by Second-Harmonic and Sum-Frequency Generation. Nature1989, 337, 519−525.
(13) Zheng, D.; Lu, L.; Li, Y.; Kelly, K. F.; Baldelli, S. Compressive Broad-Band Hyperspectral Sum Frequency Generation Microscopy to Study Functionalized Surfaces. J. Phys. Chem. Lett. 2016, 7, 1781− 1787.
(14) Zheng, D.; Lu, L.; Kelly, K. F.; Baldelli, S. Chemical Imaging of Self-Assembled Monolayers on Copper Using Compressive Hyperspectral Sum Frequency Generation Microscopy. J. Phys. Chem. B2017, 122, 464−471.
(15) Cai, X.; Hu, B.; Sun, T.; Kelly, K. F.; Baldelli, S. Sum Fequency Generation-Compressive Sensing Microscope. J. Chem. Phys. 2011, 135 (19), 194202.
(16) Santos, G. M.; Baldelli, S. Monitoring Localized Initial Atmospheric Corrosion of Alkanethiol-Covered Copper Using Sum Frequency Generation Imaging Microscopy: Relation between Monolayer Properties and Cu 2O Formation. J. Phys. Chem. C2013, 117 (34), 17591 −17602.
(17) Gellman, A. J. Vapor lubricant transport in MEMS devices. Tribol. Lett. 2004, 17, 455−461.
(18) Wasan, D. T.; Nikolov, A. D. Spreading of nanofluids on solids. Nature2003, 423, 156−159.
(19) Felhösi, I.; Kalma′n, E.; Po′czik, P. Corrosion protection by self-assembly. Russ. J. Electrochem. 2002, 38, 230−237.
(20) Sun, Z.; Zheng, D.; Baldelli S. Study of the Wetting of Paraffin Films on the Metal Surface in the Dynamic Dip-Coating Process Using Compressive-Sensing Sum Frequency Generation Microscopy. J. Phys. Chem. C2018, 122, 26543−26553.
(21) Uosaki, K.; Yamada, R. Formation of two-dimensional crystals of alkanes on the Au (111) surface in neat liquid. J. Am. Chem. Soc. 1999, 121, 4090−4091.
(22) Xie, Z. X.; Xu, X.; Mao, B. W.; Tanaka, K. Self-assembled binary monolayers of n-alkanes on reconstructed Au (111) and HOPG surfaces. Langmuir2002, 18, 3113−3116.
(23) Zhang, H.-M.; Xie, Z.-X.; Mao, B.-W.; Xu, X. Self-assembly of normal alkanes on the Au (111) surfaces. Chem. Eur. J. 2004, 10, 1415−1422.
(24) Yoshimura, D.; Ishii, H.; Ouchi, Y.; Ito, E.; Miyamae, T.; Hasegawa, S.; Okudaira, K. K.; Ueno, N.; Seki, K. Angle-resolved ultraviolet photoelectron spectroscopy and theoretical simulation of a well-ordered ultrathin film of tetratetracontane (n-C44H90) on Cu (100): Molecular orientation and intramolecular energy-band dispersion. Phys. Rev. B: Condens. Matter Mater. Phys. 1999, 60, 9046−9060.
(25) Endo, O.; Nakamura, M.; Amemiya, K.; Ozaki, H. Compression Induced Conformation and Orientation Changes in an n-Alkane Monolayer on a Au (111) Surface. Langmuir2017, 33, 3934−3940.
(26) Yamamoto, M.; Sakurai, Y.; Hosoi, Y.; Ishii, H.; Kajikawa, K.; Ouchi, Y.; Seki, K. Structures of a Long-Chain n-Alkane, n-C44H90, on a Au(111) Surface: An Infrared Reflection Absorption Spectroscopic Study. J. Phys. Chem. B2000, 104, 7363−7369.
(27) Bagus, P. S.; Weiss, K.; Schertel, A.; Wöll, C.; Braun, W.; Hellwig, C.; Jung, C. Identification of transitions into Rydberg states in the X-ray absorption spectra of condensed long-chain alkanes. Chem. Phys. Lett. 1996, 248, 129−135.
(28) Marchenko, O.; Cousty, J. Molecule length-induced reentrant self-organization of alkanes in monolayers adsorbed on Au (111). Phys. Rev. Lett. 2000, 84, 5363−5366.
(29) Marchenko, A.; Lukyanets, S.; Cousty, J. Adsorption of alkanes on Au (111): Possible origin of STM contrast at the liquid/solid interface. Phys. Rev. B: Condens. Matter Mater. Phys.2002, 65, 045414.
(30) Rabe, J. P.; Buchholz, S. Commensurability and mobility in two-dimensional molecular patterns on graphite. Science1991, 253, 424−427.
(31) Morishige, K.; Takami, Y.; Yokota, Y. Structures of alkanes and alkanols adsorbed on graphite in solution: Comparison with scanning tunneling-microscopy images. Phys. Rev. B: Condens. Matter Mater. Phys. 1993, 48, 8277−8281.

THE DEVELOPMENT OF SECCM

FEATURED INTERVIEW

AN INTERVIEW WITH DR. MARTIN EDWARDS UNIVERSITY OF UTAH

How was the SECCM technique developed?

It is said that 'necessity is the mother of all invention'- the development of scanning electrochemical cell microscopy (SECCM) was no exception. It was developed during my PhD in the group of Prof. Pat Unwin (University of Warwick, UK), out of the desire to answer a scientific question, which was beyond the reach of existing technology. Specifically, we wanted to measure the rates of electrochemical reactions on heterogeneous surfaces, where the heterogeneity was on ~10 nm-1 μm length scale.

In a conventional electrochemical measurement, the entire sample is immersed in solution and the current reports the total rate of electron-transfer occurring over the entire sample. Clearly this is no good if you want to understand the heterogeneity, so we turned to scanned probe microscopy.

At the time, the state-of-the-art in electrochemical scanned probe microscopy involved immersing the entire sample in electrolyte and scanning a microelectrode in close proximity to it. The current at the microelectrode reports the local concentration of electrochemically active species, from which a map of the reactivity of the underlying substrate is inferred.

Scanned microelectrodes had been used to quantify heterogeneity in physical and biological systems ranging from respiration in cell cultures, through electrocatalysis, to corrosion in alloys. However, these techniques had some shortcomings: (1) the current measured depends on both the microelectrode-to-sample distance and the rate of the electrochemical reaction on the sample surface;to accurately determine the rate alone requires considerable expertise and careful experimental design.(2) Spatial resolution is diminished by diffusion of reaction products, and quantification of rates in low activity regions is obscured by the reaction product from nearby active regions.

SECCM simultaneously overcomes these two challenges. The meniscus at the end of a micro- or nanopipette, when touched to the substrate surface, defines the region in which the electrochemical reaction takes place. There is no diffusion from neighboring regions, as they are not in solution. Moreover, as the current measured comes only from the wetted region, we have a direct measure of the rate of the electrochemical reaction in that region, with no need for complex analysis.

The development of SECCM did not occur in isolation. Fortunately, the Unwin lab (Warwick, UK), where the instrument was developed, already had the physical components from other electrochemical scanned probe microscopes, which were capable of precise positioning and the measurement of small currents. The lab had also previously experimented with electrochemistry in ~100 μm diameter droplets, which was achieved by hand-positioning the meniscus at the end of a capillary to the surface using manual micro-positioners and a video microscope. SECCM grew from combining these two techniques.

Switching to using an electrochemical signal to detect contact of the meniscus with the surface meant we no longer relied on the video microscope. We could then use much smaller(~100 nm) pipettes, a ~4 orders of magnitude improvement in resolution! Since then, the lateral resolution of the technique has continued to improve, with 10's nm lateral resolution imaging reported.

To stop the movement of the pipette once the meniscus made contact with the surface and before the pipette would crash into the surface would take super-human reactions, so I programmed an instrument to do it. Fortunately, it worked out! The instruments today still operate on the same basic principles we developed. However, while the first images ~10 years ago took 2-3 hours and only contained ~400 pixels (20×20), the state-of-the-art - acquiring an image with 10,000+ pixels in only 10 mins – is testament to the hard work of numerous graduate students and postdocs who have continued to refine the technique.

From the humble beginnings of one instrument and a couple of different applications, it has been gratifying to see the spread of SECCM to other research groups. The Unwin lab continue to be pioneers in developing instrumentation, theory and applications. However, in a relatively short period, there has been rapid uptake by the community - off the top of my head I can think of at least 15 groups who have adopted the technique, and I'm in no doubt that there are several more.

What are the main advantages of the SECCM technique?

SECCM provides a straight forward way to map the electrochemistry and topography of their samples with nanoscale resolution. The experiments are not difficult to perform, the probe for SECCM (micro- or nanopipettes) can be cheaply (~$1) and rapidly (~1 min) fabricated from a glass or quartz capillary with very little expertise. Indeed we have had high-school students visit the lab and become competent in their fabrication in only 15 minutes. Interpretation is simple – a higher current represents a higher rate of the electrochemical reaction in the region probed.

The SECCM is a versatile technique. The experimenter is free to choose the chemical system they investigate be altering composition of the solution they fill their pipette with and there is little need for special preparation of samples. Moreover, after the meniscus contacts the surface and defines the electrochemical cell (hence the name of the technique), the experimenter is free to apply the electroanalytical technique that is most appropriate to questions they are asking.

Each time the meniscus touches the sample is the first time that region has seen the electrolyte and can be treated as a new experiment. This makes 10,000 experiments on a single sample a viable possibility, offering exciting possibilities in high-throughput experimentation.

Do you think that SECCM is an important application for researchers and why?

For researchers looking to gain insight into heterogeneity of electrochemical materials, SECCM is a great technique, to which there are very few alternatives. As all electrodes are heterogeneous at some level, the range of systems that it can be applied to is incredibly broad. The measurements made are clear-cut and don't rely on convoluted analyses. Moreover, when coupled with complementary techniques, one can correlate electrochemical activity with structure, which is the Holy Grail in the field of electrocatalysis.

SECCM allows one to characterize the boundaries between different regions on an electrode surface, which are frequently the location for interesting behaviors. For example, in a recent collaboration with Matt Kanan's group (Stanford), we recently visualized enhanced CO_2 reduction activity at grain boundaries on polycrystalline Au (https://doi.org/10.1126/science.aao3691). Matt had a hunch that this was the case, due to a correlation between the density of boundaries and the activity, but had no direct evidence. SECCM changed this, giving us the opportunity to literally see the current increase over the grain boundaries.

While predicting the future in any field is a fool's errand, if we take the ever-expanding body of literature as a clue, it seems that the only limitation in the application of SECCM is the creativity of scientists and engineers. Personally, I'm particularly excited to see SECCM push forward understanding in energy technologies, such as batteries and fuel cells, where materials are complex composites.

How was your experience working with Park Systems on developing this technique?

Working with Park Systems has been a collaborative endeavor. The R&D team we work with are a talented team of engineers, but had limited chemical experience. Thus our first task was to deliver a crash course in electrochemistry. Thankfully, they are fast learners!

Park's experience in both AFM and SICM reassured us that we would be able to perform low mechanical and electrical noise measurements. Fortunately, that the hardware (tip holder & amplifier) for SICM and SECCM are interchangeable, thus the effort in adapting the instruments to perform SECCM has been focused in software. This has involved implementing new control algorithms and ways of presenting the acquired data. Thankfully, through the hard work of all involved, we now perform high quality SECCM imaging on our NX-12 instrument.
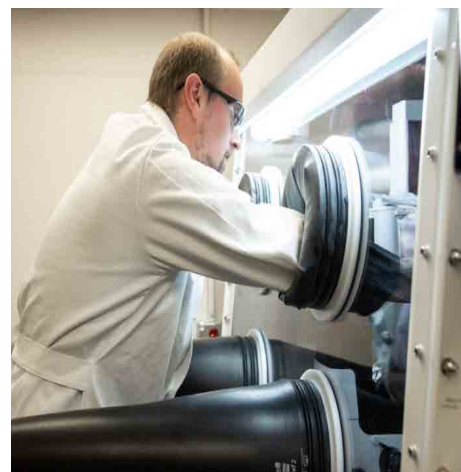
Dr. Martin Andrew Edwards
is currently a Research assistant professor at the University of Utah. He completed his PhD under supervisors Prof. P.R. Unwin and Dr. A.L. Whitworth, University of Warwick, Molecular Organisation and Assembly in Cells Doctoral Training Centre (MOAC DTC)–Thesis title: *Development of electrochemical probe microscopy and related techniques* in 2009. He currently has funding from DURIP - Environmental Electrochemical Scanned Probe Microscope for Investigating Nanoscale Phase Behavior and 3-Phase Boundaries and funding pending at the Department of Energy - Molecular Interrogation of Concerted Electron- and Phase-Transfer Reactions. He has been invited to present at many conferences including "Electrochemistry at three-phase boundaries" ACS Spring meeting; "Resistive Pulse Delivery of Single Nanoparticles to Electrochemical Interfaces" Pittcon, Chicago; "Nanoparticle Dynamics at Electrified Interfaces" Society of Western Analytical Professors (SWAP) Meeting, Salt Lake City; "Single Entity Electrochemistry", invited seminar, University of Warwick; and "Electrochemistry of Nanobubbles" Utah Energy Symposium, Salt Lake City.
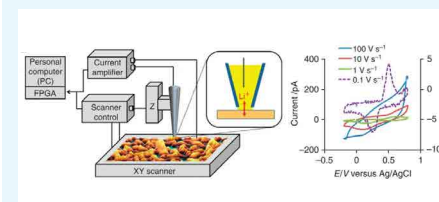
SECCM is a promising technique for measuring the heterogeneity in Li+ insertion into battery cathodes. (above) schematic of SECCM setup

HIGH RESOLUTION IMAGING OF PARTICLES DISPERSED IN POLYMERIC MATRIX BY TRUE NON-CONTACT™ MODE ATOMIC FORCE MICROSCOPY

John Paul Pineda, Gabriela Mendoza, Cathy Lee, Byong Kim, and Keibock Lee - Park Systems Inc.

Introduction

Nanoscale materials, or nanoparticles, have received increasingly more research attention as compared to similar macroscale materials because of their unique properties. They include an exceptionally high surface area to volume ratio, and an extensive interface between the matrix and the reinforcement material [1-3]. There are numerous emergent applications that require the dispersion of nanoparticles into a polymeric matrix; the most common of these applications are biomedical sciences, piezoelectric actuators and sensors, microelectronic devices, capacitors and even smart materials [1, 3-5]. Nanoparticles are dispersed into a polymeric matrix to enhance and improve the properties of composite material. For example, the presence of barium titanate ($BaTiO_3$) nanoparticles in thermosetting polymer composites enhances the piezoelectric, ferroelectric, and pyroelectric properties of these systems [1]. Incorporating other types of nanoparticles may enhance or improve optical properties, heat resistance or mechanical properties such as stiffness, strength and resistance to wear and damage of the composite materials [2, 6]. Particle and agglomeration size and dispersion of nanoparticles in polymer matrices play a crucial role in describing the ultimate performance of the composite material [2, 6-8]. Šupová et al. reported that particle agglomerates decrease material performance by the inclusion of voids that act as preferential sites for crack initiation and failure [2]. For this reason, a technique that can generate images of sufficient resolution to visualize particle and agglomeration dispersion, and accurately measure their sizes, is critically important. Atomic Force Microscopy (AFM) is one of the more common methods utilized in previous studies to characterize this type of nanomaterial utilizing a semi-contact or "tapping" mode [9, 10]. In this technique, the tip oscillates near its resonance frequency, allowing the tip to periodically touch the sample surface. According to Hanemann et al., nanoparticles form soft or hard agglomerates depending on the synthesis conditions and the surface chemistry. Soft agglomerates can be degraded into smaller particles by shear forces generated by mechanical stress gradients [5]. Since the tapping mode requires a tip-to-sample interaction, it is possible that the scanning might alter particle distributions of soft agglomerates, and lead to inaccurate data. The True Non-Contact™ imaging mode of AFM systems from Park Systems allows the acquisition of surface topography without the AFM tip touching the sample. The advanced Z scanner design of Park AFM is the key feature in achieving the non-contact imaging performance that defines Park's True Non-Contact mode – producing the best image resolution and accurate topographical data, while maintaining the tip sharpness and minimizing the chance of damaging or altering the sample surface [11]. In this paper, two different samples with nano- and microparticles dispersed in polymeric matrices were studied. High resolution topography images were obtained with accurate measurement and evaluation of particle/agglomerate sizes was done using Park NX10 True Non-Contact™ mode.

Experimental

Two different samples were investigated using a Park NX10 AFM system. The samples were cotton filter-like substances with nano- and micron-sized particles dispersed in a polymeric matrix. Both samples were placed between two flat metal disks. The samples were gently pressed together from both sides of the metal disks to compress and planarize the sample surface. Subjected to gentle finger pressure, the samples were less fluffy and substantially more planar. A silicon tip based cantilever probe was used for the measurement of both samples. The topography of the samples was obtained using the True Non-Contact™ mode of Park Systems. In non-contact mode, the topography image was acquired by measuring the changes in the vibrational amplitude of the cantilever induced by attractive van der Waals forces as the cantilever mechanically oscillated near its resonant frequency during the scan. The measured changes are compensated by the AFM's feedback loop, which maintains a constant cantilever amplitude and distance. Non-contact mode measures the topography of the sample surface by using this feedback mechanism to control the Z scanner movement [12].

Results and Discussion

Figure 1 shows the topography images acquired from Sample 1. The topography with enhanced color image representations show different features available in the sample surface, which includes the polymeric matrix background, as well as individual and agglomerated particles of varying sizes. The polymeric matrix background of Sample 1 was relatively flat. Also, the particles distributed in the polymer matrix have a variety of sizes with the larger particles potentially composed of agglomerated smaller particles. The small particles range in size from 1–3 µm nominally, while bigger aggregates are approximately 10 microns wide. Figure 1b shows an enlarged section from Figure 1a that features two microparticles, both of which appear to be faceted (i.e., having sides with well-defined shapes). The particle on top has an elongated shape while the bottom particle features a more rounded shape. Both particles have octagonal features with lengths of approximately 1.0 µm and 0.5 µm in height. A line profile analysis was also performed using Park XEI image analysis software to evaluate particle sizes. The equivalent line profiles of Figure 1b are presented in Figures 1d–f. The measured widths of both particles are approximately 0.8–1.4 µm with heights between 0.35–0.5 µm.
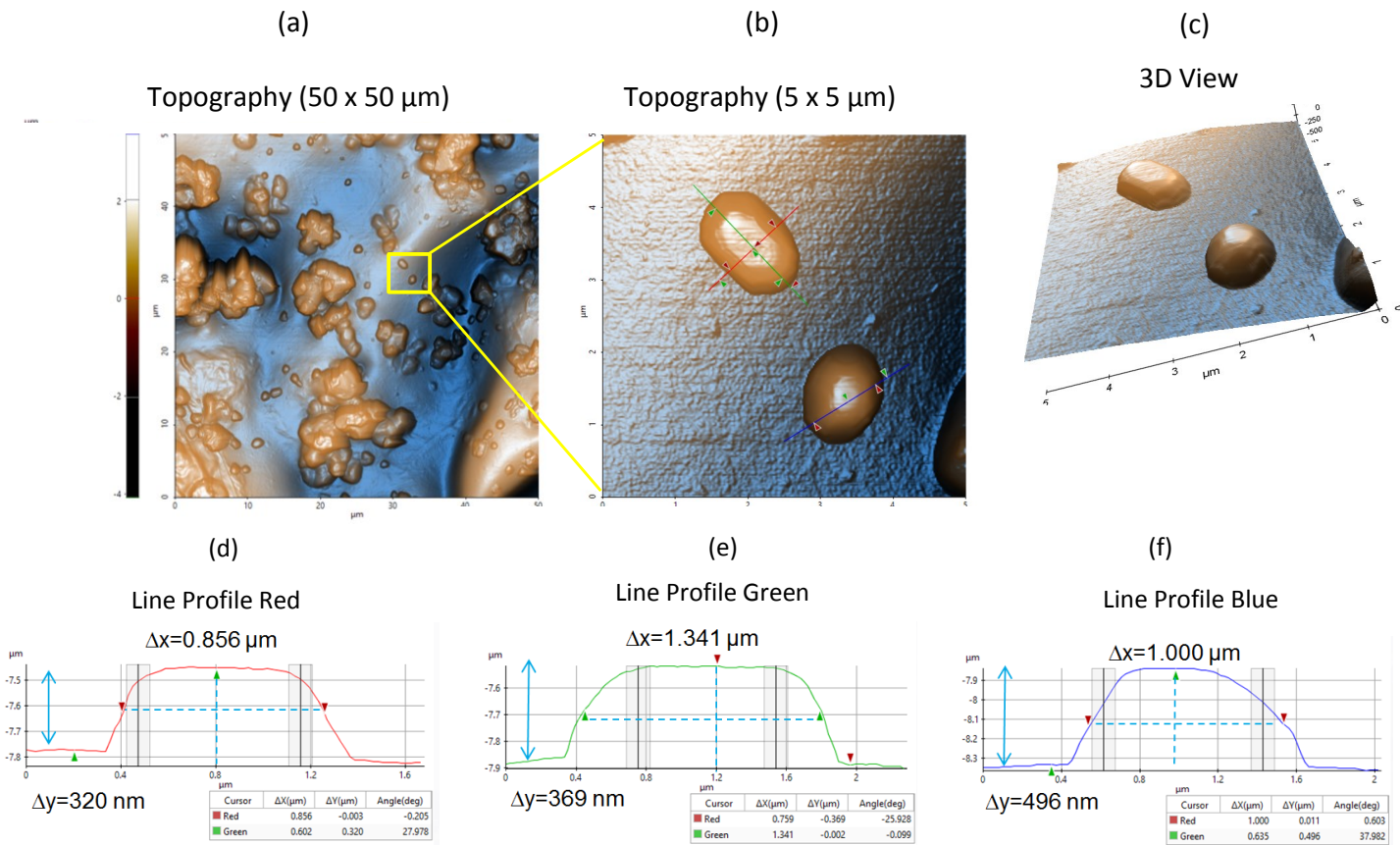
Figure 1. Topography images and line profiles of sample 1. (a) Non-contact topography AFM image. Scan Size: 50 x 50 µm, image size: 512 x 512 pixels. (b) Zoom in view of topography inside the yellow box in Figure 1a. Scan size: 5 x 5 µm, image size: 256 x 256 pixels. (c) Corresponding 3D view of Figure 1b. (d-f) Corresponding line profiles of Figure 1b.
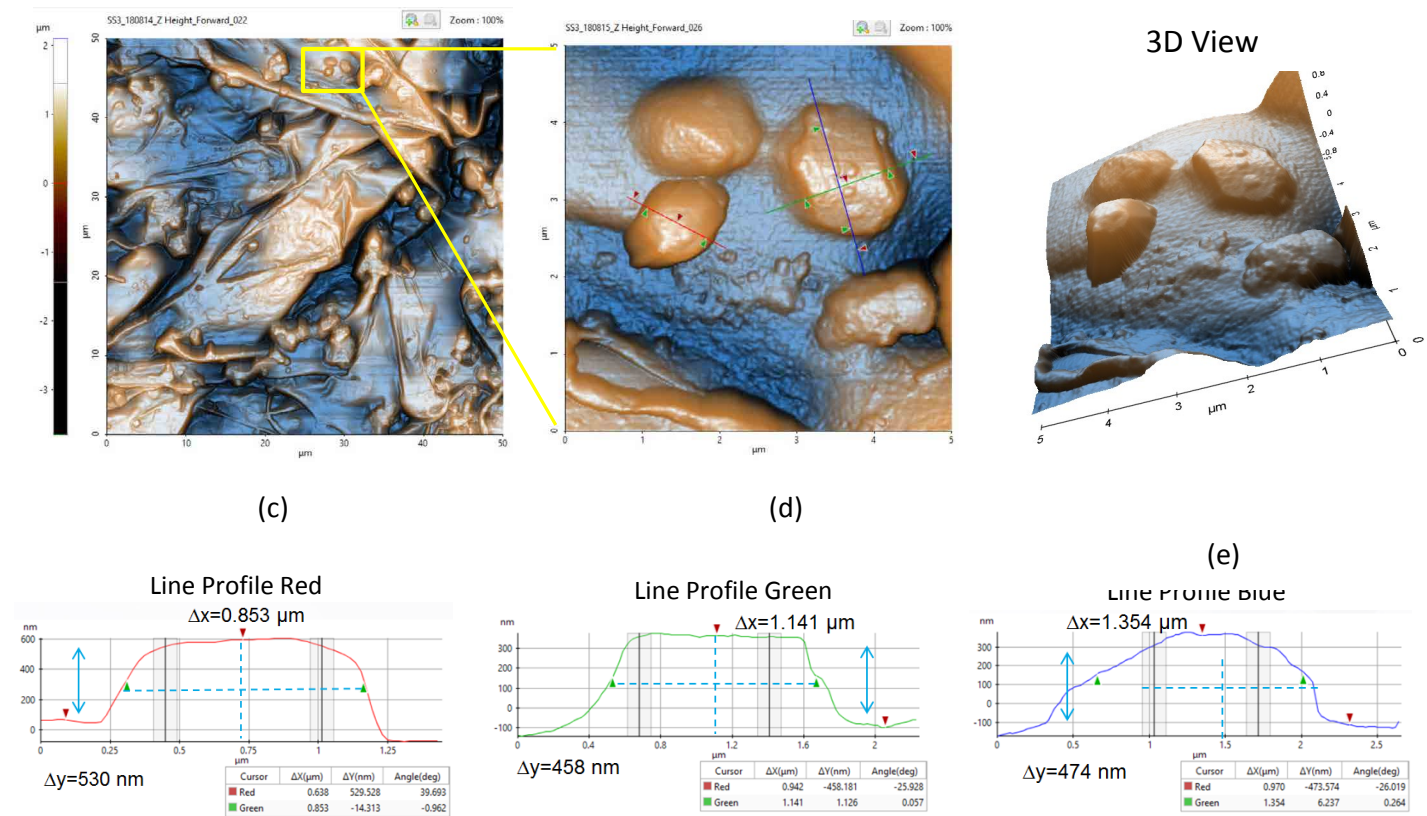

Figure 2. Topography images and line profiles of Sample 2. (a) Non-contact topography AFM image. Scan Size: 50 x 50 µm, image size: 512 x 512 pixels. (b) Zoom in view of topography inside the yellow box in Figure 2a. Scan size: 5 x 5 µm, image size: 256 x 256 pixels. (c) Corresponding 3D view of Figure 2b. (d-f) Corresponding line profiles of Figure 2b.

Figure 2 represents the topography and line profile acquired from Sample 2. This 50 x 50 µm region shows an uneven surface of the polymeric background. Individual particles and agglomerates of varying sizes were also observed. Figure 2b shows an enlarged section from Figure 2a and features four well-defined individual microparticles. Each particle appears to be facetted with hexagonal features, with nominal dimensions of 1.0 µm in length and 0.5 µm in height. The equivalent line profiles from Figure 2b are presented in Figures 2d–f. The measured particle widths were approximately 0.8–1.4 µm, with heights of approximately 0.5 µm.

Grain analysis, the straightforward and simultaneous size quantification of many particles, was also performed using Park XEI software. In grain analysis, the particles selected for size calculation were chosen by adjusting the scroll bar on the Histogram Graph. Table 1 shows detailed information of all grains detected from the NCM topography image from Sample 1 (which is shown in Figure 3). The grain analysis table contains multiple dimensional parameters such as length, area and volume, as well as mean and standard deviation values of tabulated grains. The average size of particles shown in Figure 3 was calculated as 1.390 µm ± 0.148 µm. Figure 4 shows the grain analysis data of Sample 2 with a calculated average particle size of 1.492 µm ± 0.217 µm. All particles measured in these experiments were in the micrometer range; the lack of individual and detectable nanoscale particles strongly suggests that any nanoscale particles were incorporated into larger agglomerates, or microscale clusters. Nanoscale particles tend to form agglomerates due to the strong and dominant van der Waals forces between them [2].

Conclusion

The particles dispersed in polymeric matrices of two different samples were well characterized using True Non-Contact™ mode on a Park NX10 AFM system. This technique acquired surface topography without the AFM tip touching the sample, which minimizes the chance of damaging or altering the sample surface. The high resolution images obtained in the experiment allowed the accurate measurement and evaluation of particle sizes and distribution within the polymer matrix.
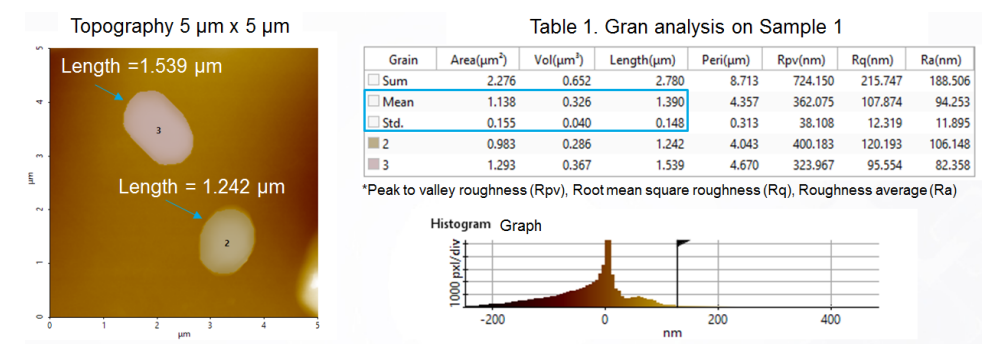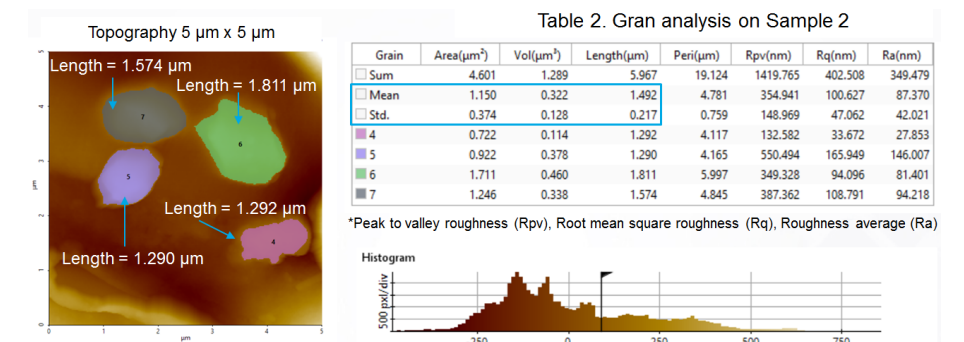

Figure 3. Grain size analysis data of Sample 1.

Table 1. Gran analysis on Sample 1

Grain	Area(µm²)	Vol(µm³)	Length(µm)	Peri(µm)	Rpv(nm)	Rq(nm)	Ra(nm)
Sum	2.276	0.652	2.780	8.713	724.150	215.747	188.506
Mean	1.138	0.326	1.390	4.357	362.075	107.874	94.253
Std.	0.155	0.040	0.148	0.313	38.108	12.319	11.895
2	0.983	0.286	1.242	4.043	400.183	120.193	106.148
3	1.293	0.367	1.539	4.670	323.967	95.554	82.358

*Peak to valley roughness (Rpv), Root mean square roughness (Rq), Roughness average (Ra)

Figure 4. Grain size analysis data of Sample 2.

Table 2. Gran analysis on Sample 2

Grain	Area(µm²)	Vol(µm³)	Length(µm)	Peri(µm)	Rpv(nm)	Rq(nm)	Ra(nm)
Sum	4.601	1.289	5.967	19.124	1419.765	402.508	349.479
Mean	1.150	0.322	1.492	4.781	354.941	100.627	87.370
Std.	0.374	0.128	0.217	0.759	148.969	47.062	42.021
4	0.722	0.114	1.292	4.117	132.582	33.672	27.853
5	0.922	0.378	1.290	4.165	550.494	165.949	146.007
6	1.711	0.460	1.811	5.997	349.328	94.096	81.401
7	1.246	0.338	1.574	4.845	387.362	108.791	94.218

*Peak to valley roughness (Rpv), Root mean square roughness (Rq), Roughness average (Ra)

In summary, the True Non-Contact™ mode provides researchers with the means to characterize sample surfaces on the nanoscale level with high resolution and accuracy, without interference from tip blunting or tip-induced sample damage.

References

1. Asimakopoulos I, et al., Nanocomposites of Barium Titanate Nanoparticles Embedded in Thermosetting Polymer Matrices (Novolac Resin/Unsaturated Polyesters/Epoxy Resin): A Comparative Study. February 2019. DOI: 10.3390/chemengineering3010012.
2. Šupová M, et al., Effect of Nanofillers Dispersion in Polymer Matrices; A Review. Science of Advanced Materials Vol. 3, 1–25, 2011
3. Okpala C., THE BENEFITS AND APPLICATIONS OF NANOCOMPOSITES. Okpala, International Journal of Advanced Engineering Technology.
4. Corbierre M., et al., Polymer-Stabilized Gold Nanoparticles and Their Incorporation into Polymer Matrices. J. Am. Chem. Soc., 2001, 123 (42), pp 10411–10412. DOI: 10.1021/ja016628.
5. Hanemann T., et al., Polymer-Nanoparticle Composites: From Synthesis to Modern Applications. Materials 2010, 3, 3468-3517; doi:10.3390/ma3063468.
6. Mrlik M., Fillers in advanced nanocomposites for energy harvesting. Fillers and Reinforcements for Advanced Nanocomposites, 2015.
7. Zhang R., Entropy-driven segregation of polymer-grafted nanoparticles under confinement.
8. Schlabach S., et al., Nanoparticles in polymer-matrix composites. Microsystem Technologies February 2011, Volume 17, Issue 2, pp 183–193.
9. RAMAZANOV M., THE MAGNETIC POLYMER NANOCOMPOSITE MATERIALS BASED ON POLYPROPYLENE AND IRON NANOPARTICLES: SYNTHESIS AND STRUCTURE. Journal of Ovonic Research Vol. 12, No. 4, July - August 2016, p. 193 – 200.
10. Tanaka T., et al., Tailoring of Nanocomposite Dielectrics: From Fundamentals to Devices and Applications.
11. Pineda J., et al., True Non-Contact Imaging of Various Samples. Retrieved March 03, 2019, from https://www.parksystems.com/index.php/applications/life-science/micro-and-molecular-biology/702-true-non-contact-imaging-of-various-samples?highlight=WyJqb2huliwicGF1bCIsImpvaG4gcGF1bCJd
12. Park AFM Modes and Techniques. (n.d.). Retrieved October 18, 2016, from http://www.parkafm.com/index.php/park-afm-modes

Park Systems AFM - Highest Resolution, Accuracy and Ease of Use Brilliantly Combined

Park Systems creates the world's most accurate line of nanoscale microscopy and metrology tools for research and industrial applications. Our innovation features, such as True-Non Contact™ mode and cutting-edge automation, set our products apart from the competition and make Park Systems AFMs the easiest to use and most advanced AFMs available.

To find out more, please email us at inquiry@parksystems.com or visit us at www.parksystems.com

General AFMs

Park Systems provides a range of popular AFMs for general research and industrial applications. Designed to be extremely versatile while still providing the accuracy and functionality necessary to do high quality work, our line of general AFMs offer researchers and engineers alike the ability to get extremely accurate results quickly and easily.

Applications:

- Biological Science
- Materials Science
- Failure Analysis
- Semiconductor Analysis
- Hard Disk Media Analysis

Small sample AFM

Park XE7
True research-grade AFM for the practical budget

Park NX10
The world's most accurate easy-to-use research AFM

Park NX-Hivac
The most advanced high vacuum AFM for failure analysis and sensitive materials research

Large sample AFM

Park XE15
Capable, adaptable, and affordable-the best value large sample AFM

Park NX20
Power, versatility, ease of use, brilliantly combined for large sample AFM

Park NX20 300mm
The leading automated nanometrology tool for 300 mm wafer measurement and analysis

Bio and Chemical

Biological research is one of the fastest growing fields of the 20th century. Park AFMs have played critical roles in this sector, giving researchers the tools they need to develop novel insights into the vast and complicated processes and structures of biology.

Park NX10 SICM
Cutting-edge nanoscale imaging in aqueous environments

Park NX12-Bio
Three compelling nanoscale microscopies in one innovative platform

Park NX12
The most versatile AFM for analytical and electrochemistry

Industrial AFMs

Park Systems is dedicated not just to advancing research, but industry as well. That's why our designers have worked to build a line of the most effective AFMs for FA engineers and industrial applications. Allowing users to take highly accurate measurements and complete their work more quickly, these tools can improve efficiency in the workplace and reduce errors, leading to a more profitable, more consistent development and production process.

Applications:

- Failure Analysis
- Semiconductor Analysis
- Hard Disk Media Analysis

Park NX-HDM
The most innovative AFM for automated defect review and surface roughness measurement

Park NX-PTR
Fully automated AFM for accurate inline metrology of hard disk head sliders

Park NX-Wafer
Low noise, high throughput atomic force profiler with automatic defect review

Park NX-3DM
Innovation and efficiency for 3D metrology

ATOMIC FORCE MICROSCOPE (AFM)-BASED NANOMANUFACTURING ASSISTED BY VIBRATION AND HEAT

Jia Deng, Asst. Professor, Dept. of Systems Science and Industrial Engineering at Binghamton University

Introduction

Maskless nanolithography techniques are critical to fabricate masks and molds for mass production, low volume nanodevices, and various research areas. Atomic force microscope (AFM)-based nanomanufacturing, as an emerging low-cost and easy-to-setup maskless nanomanufacturing technique, enables comparable resolution to that of electron beam lithography, which is commonly used for fabricating masks for photolithography and arbitrary nanopatterns.

Different AFM-based nanomanufacturing approaches, such as mechanical direct scratching[1], dynamic plowing[2], thermal-mechanical material removing[3], electrostatic nanolithography[4], and dip-pen nanolithography[5], have been developed as advanced tip-based nanomanufacturing techniques. However, for most existing material removal approaches, the dimensions of nanopatterns are defined by the tip size, which limits the nanomanufacturing capabilities and efficiency. Moreover, relatively large forces are often associated with material removal processes. For example, mechanical scratching commonly requires micro-Newton level normal forces to modify surfaces, which leads to quick tip wear and degraded pattern fidelity[6]. Thermal-mechanical technique often needs special thermal probes to implement the technique, although with lower normal force in the range of a few hundreds of nano-Newtons[3].

To easily control the dimensions of nanopatterns and reduce the normal forces, we integrated mechanical vibration and sample heating in the AFM-based nanomanufacturing process[7]. With mechanical vibration, dimensions of nanopatterns can be controlled. The elevated temperature enables a nanomanufacturing process using only tens of nano-Newtons normal forces. Results demonstrated the functions of mechanical vibration and sample heating on enhancing the AFM-based nanomanufacturing capabilities and performances.
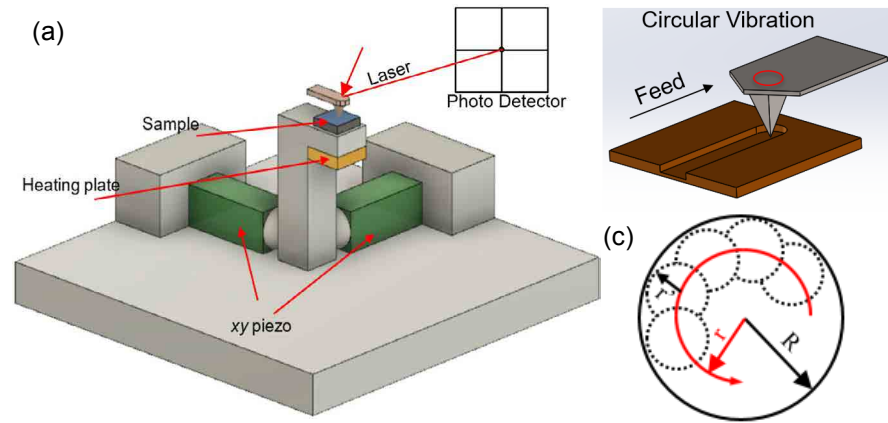

Figure 1. (a) Schematic illustration of the experimental setup for AFM-based nanomanufacturing assisted by vibration and heat. (b) Mechanism of fabricating nanopatterns with controlled width. (C) Schematic illustration of actual feature width, which comprises the vibrational amplitude and the tip diameter.

Experimental Setup

The experimental setup includes a commercially available AFM from Park Systems (XE-7) and an in-house fabricated nanomanufacturing stage that integrates the mechanical vibration and thermal energy into the nanomachining process, as shown in Figure 1(a). Two perpendicularly placed piezoelectric actuators generate circular vibration on the sample through the center pillar when the driving sinusoid signals for them have the same amplitude, but 90-degree phase difference. Figure 1(b) illustrates that the circular sample vibration controllably defines the actual dimensions of nanopatterns by simply changing the vibrational amplitude. Figure 1(c) shows the virtual tool radius R, which is the sum of the tip radius r' and the vibrational amplitude r. AFM tips used for nanomanufacturing were DLC190 and CSG10/Au.

In addition to the vibration, the heating element generates the thermal energy on samples. AFM tips can penetrate through the sample surface easier under elevated temperature than that of no heating because the sample we use in this nanomanufacturing scenario is a thermoplastic material polymethyl methacrylate (PMMA). The sample temperature is positively related to the DC voltage applied to the heating element, and the specific values were calibrated using a thermometer.

For the manufacturing process, vectors and bitmap images can be designed and fabricated on PMMA surfaces by utilizing the lithography software. Forces or height information can be assigned to the vectors and bitmap images to fabricate two dimensional and three dimensional nanopatterns with this experimental setup.

Results and Discussions

2D and 3D nanopatterns can be controllably fabricated using the aforementioned AFM-based nanomanufacturing setup[8], [9]. Figure 2 demonstrated that in-plane vibration can effectively tune the dimension of nanopatterns by setting different vibrational amplitude without the limitation of the tip size. Nanopatterns with different widths, 86 nm, 116 nm, and 151 nm in this case, can be fabricated by one single path, which enhances the nanomanufacturing efficiency and capability.

In addition to 2D nanopatterns, 3D shapes can also be fabricated. Figure 3 shows the grayscale bitmap template image and 3D results on PMMA[10]. The results showed that the nanomanufacturing capability of fabricating arbitrary 3D nanopatterns by the vibration-assisted AFM-based nanomanufacturing.

Sample heating was utilized to further decrease the normal force needed for fabricating patterns so as to decrease the
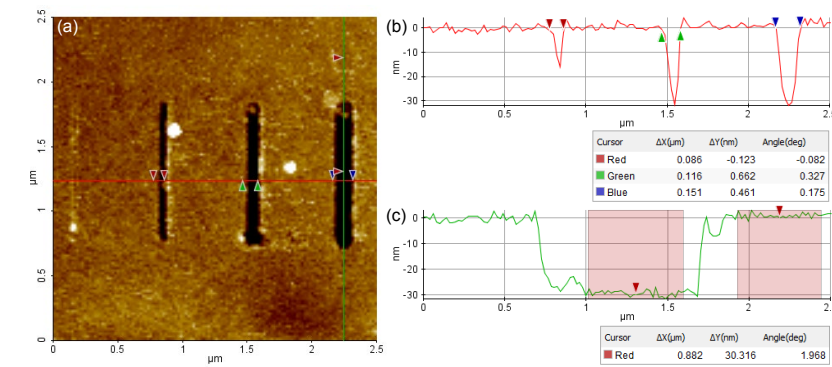

Figure 2: (a) 2D nanopatterns fabricated by employing the in-plane vibration. (b) Cross-sectional profile of all nanopatterns. (C) Cross-sectional profile of the last nanotrench.
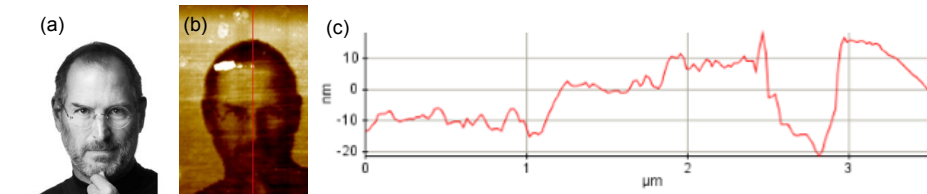

Figure 3: (a) Grayscale bitmap template image of Steve Jobs [11]. (b) 3D nanopatterns fabricated the AFM-based nanomanufacturing process [10]. (c) Cross-sectional profile of the result.
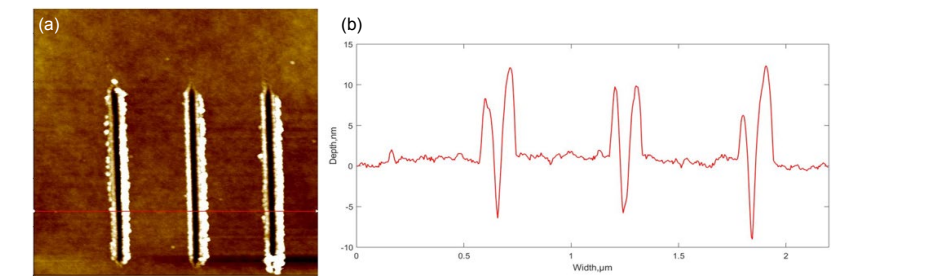

Figure 4: (a) Topography and (b) cross-sectional profile of nanotrenches fabricated by AFM-based nanomanufacturing assisted by vibration and heat using a soft tip CSG10/Au, of which the nominal spring constant is 0.11 N/m.

tip wear. When the sample surface is slightly heated up to 42°C, a very small normal force of 50 nN can generate nanopatterns, as shown in Figure 4. The tip used for the nanopatterning was very soft CSG10/Au with the nominal spring constant of 0.11 N/m, which is very difficult, if not impossible at all, for nanopatterning in other tip-based nanomanufacturing techniques. The widths and depths of the fabricated nanotrenches are about 45 nm and 8 nm, respectively. We demonstrated that nanopatterns with high fidelity can be fabricated by our proposed AFM-based nanomanufacturing assisted by both vibration and heat.

Summary

Vibration and thermal energy assisted AFM-based nanomanufacturing can be used to fabricate two dimensional and arbitrary three dimensional nanopatterns for numerous applications. The in-plane vibration provides tunable feature dimensions and higher nanopatterning efficiency. The required normal forces for the nanomanufacturing are reduced to the level of tens of nano-Newtons because the thermal energy applied on the thermoplastic sample softens the sample. Integration of the vibration and heat in the AFM-based nanomanufacturing process enhances the nanopatterning capabilities and performances.

References
[1] R. Rank, H. Brückl, J. Kretz, I. Mönch, and G. Reiss, "Nanoscale modification of conducting lines with a scanning force microscope," Vacuum, vol. 48, no. 5, pp. 467–472, May 1997.
[2] B. Klehn and U. Kunze, "Nanolithography with an atomic force microscope by means of vector-scan controlled dynamic plowing," Journal of Applied Physics, vol. 85, no. 7, pp. 3897–3903, Mar. 1999.
[3] D. Pires et al., "Nanoscale Three-Dimensional Patterning of Molecular Resists by Scanning Probes," Science, vol. 328, no. 5979, pp. 732–735, May 2010.
[4] M. Ishibashi, S. Heike, H. Kajiyama, Y. Wada, and T. Hashizume, "Characteristics of scanning-probe lithography with a current-controlled exposure system," Appl. Phys. Lett., vol. 72, no. 13, pp. 1581–1583, Mar. 1998.
[5] D. S. Ginger, H. Zhang, and C. A. Mirkin, "The Evolution of Dip-Pen Nanolithography," Angewandte Chemie International Edition, vol. 43, no. 1, pp. 30–45, Jan. 2004.
[6] Y. Q. Geng et al., "Fabrication of millimeter scale nanochannels using the AFM tip-based nanomachining method," Applied Surface Science, vol. 266, pp. 386–394, Feb. 2013.
[7] H. Zhou, C. Dmuchowski, C. Ke, and J. Deng, "External-energy-assisted nanomachining with low-stiffness atomic force microscopy probes," Manufacturing Letters, vol. 23, pp. 1–4, Jan. 2020.
[8] J. Deng, L. Zhang, J. Dong, and P. H. Cohen, "AFM-based 3D nanofabrication using ultrasonic vibration assisted nanomachining," Journal of Manufacturing Processes, vol. 24, pp. 195–202, Oct. 2016.
[9] J. Deng, J. Dong, and P.H. Cohen, "Development and Characterization of Ultrasonic Vibration Assisted Nanomachining Process for Three-Dimensional Nanofabrication," IEEE Transactions on Nanotechnology, vol. 17, no. 3, pp. 559–566, May 2018.
[10] J. Deng, J. Dong, and P. Cohen, "High Rate 3D Nanofabrication by AFM-based Ultrasonic Vibration Assisted Nanomachining," Procedia Manufacturing, vol. 5, pp. 1283–1294, Jan. 2016.
[11] W. Isaacson, Steve Jobs. New York; Toronto: Simon & Schuster, 2011.
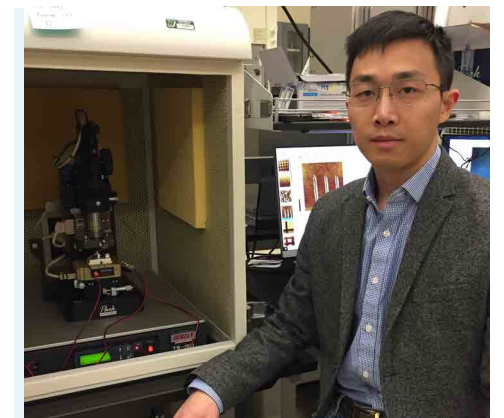
Bio:
Jia Deng joined the Department of Systems Science and Industrial Engineering at Binghamton University as an assistant professor in 2017. He received his Ph.D. degree in Industrial Engineering from North Carolina State University, 2017. He received an M.S. degree in Mechatronics Engineering from Huazhong University of Science and Technology, 2013 and a B.S. degree in Process Equipment and Control Engineering from Wuhan University of Technology, 2010. His research area is advanced manufacturing, including innovations and applications of AFM-based nanomanufacturing processes and 3D printing processes in biomedical areas. His selected publications are listed below. He recently received the Career Champion and Individual Development Award at Binghamton University.

Selected Publications:
• X. Kong, J. Deng, J. Dong, and P. H. Cohen, "Study of Tip Wear for AFM-based Vibration-Assisted Nanomachining Process," J. Manuf. Process. (Accepted)
• H. Zhou, C. Dmuchowski, C. Ke, and J. Deng*. "External-Energy-Assisted Nanomachining with Low-Stiffness AFM Probe," Manufacturing Letters, vol. 23, pp. 1–4, Jan. 2020.
• L. Mei, G. Wang, J. Deng, J. Xiao, and X. Guo. "Tunable fabrication of concave microlens arrays by initiative cooling based water droplets condensation," Soft Matter, 15, pp. 9150-9156, Oct. 2019.
• J. Deng, H. Zhou, J. Dong, and P. Cohen. "Three-Dimensional Nanomolds Fabrication for Nanoimprint Lithography," Procedia Manuf.,2019
• J. Deng, J. Dong, and P. Cohen. "Rapid Fabrication and Characterization of SERS Substrates," Procedia Manuf., vol. 26, pp. 580-586, Aug. 2018.
• J. Deng, J. Dong and P. H. Cohen, "Development and Characterization of Ultrasonic Vibration Assisted Nanomachining Process for Three-Dimensional Nanofabrication," IEEE Trans. Nanotechnol., vol. 17, no. 3, pp. 559-566, May 2018.
• G. Wang, J. Deng, and X. Guo, "Electrohydrodynamic assisted droplet alignment for lens fabrication by droplet evaporation," J. Appl. Phys., vol. 123, no. 16, p. 163102, Apr. 2018.
• J. Deng, L. Zhang, J. Dong, and P. H. Cohen, "AFM-based 3D nanofabrication using ultrasonic vibration assisted nanomachining," J. Manuf. Process., vol. 24, Part 1, pp. 195–202, Oct. 2016.
• J. Deng, J. Dong, and P. Cohen, "High Rate 3D Nanofabrication by AFM-based Ultrasonic Vibration Assisted Nanomachining," Procedia Manuf., vol. 5, pp. 1283–1294, Jan. 2016.

A GLOBAL VOICE FOR NANOTECHNOLOGY

Joining the Nanotechnology World Association means connecting to a massive global community focused on facilitating the adoption and commercialization of nanotechnology solutions across industries.

Stronger together.

THE NANOTECHNOLOGY WORLD ASSOCIATION IS LAUNCHED TO FOSTER WORLDWIDE COLLABORATION WITHIN THIS PROMISING AND HIGH GROWTH SECTOR

This new global nanotechnology association will bolster the necessary links between research and industries and facilitate the adoption and commercialization of nanotechnology in several vertical markets.

Singapore and New York, October 23rd, 2019 – The Nanotechnology World Association (NWA) has been officially launched today to execute on its mission to globally facilitate and promote adoption of nanotechnology solutions across industries by connecting entrepreneurs with researchers, start-ups with investors, suppliers with customers, employers with talents, key players with one another. The NWA is an independent, and mainly industry-oriented, advocacy group inclusive of businesses, academia, business-supporting associates, as well as affiliate government agencies and other associations.

The NWA seeks to expand and strengthen connections between stakeholders in the nanotechnology sector as these relationships are the key to fulfill the potentials of these various technologies. This will be achieved by engaging more industry members, facilitating industry-oriented programs, with an emphasis on supporting nanomanufacturing R&D projects with other educational research bodies. The NWA efforts will include the private or public spheres and active support and vigorous participation from both governments and companies is expected.

The NWA aims to expand quickly. *"We are in the process of creating chapters, to address the local needs of our members,"* said Marine Le Bouar, CEO of the NWA. *"Other plans for the Association*

include the funding of our own Institute, and the organization of the first global nanotechnology start-up competition," she added.

So far, members from North America, Europe and Asia have joined the NWA. These companies include Park Systems (South Korea) Abionic (Switzerland), Advanced Nanotechnologies (Spain), APR Technologies (Sweden), Horiba (France), Metashield (USA), nFluids (Canada), and StoreDot (Israel), among others.

"We are honored to be a founding member of Nanotechnology World Association to help promote shared knowledge amongst the growing and diverse Nano Science community. As a global leader in Atomic Force Microscopes, Park Systems is a strong advocate for collaboration to achieve nanoscale advances for the betterment of our world. " Keibock Lee, President at Park Systems (South Korea).

"Nanotech is the next frontier of material science engineering. Organizations like NWA are essential in unlocking the fundamental and transformative promise of advanced materials." Martin Ben-Dayan, CEO, Founder at Metashield LLC (USA).

"This is a much-needed initiative. As pioneers in developing nano-size materials for energy storage, we face global supply chain challenges starting from the scale up process for nano metalloids such as pure nano Silicon." Doron Myersdorf, CEO at StoreDot (Israel).

"Given the importance of nanotechnologies in the global business sphere and the huge efforts put into Research & Development, the creation of this association was long overdue."

Florian Formanek, Head of Applications, Horiba (France).

"We are happy to join forces with the Nanotechnology World Association in working on the key issues that must be addressed to successfully commercialize this vital technology." Peter Nilsson, CEO at APR Technologies (Sweden). *"In our opinion, the bridge between nanotechnology and business has yet to be built. This Association is a must-needed first step to building this bridge."* Manuel Antonio Onteniente, CEO at Advanced Nanotechnologies (Spain).

"Nanofluidics is going to disrupt the biomedical diagnostics field, by providing ultra-fast, lab-grade results from a single drop of capillary blood. The Nanotechnology World Association will aid in coordinating the key players to make this a reality soon." Dr. Nicolas Durand, PhD, Chief Executive Officer at Abionic SA (Switzerland).

About the Nanotechnology World Association
The Nanotechnology World Association (NWA) was created to help accelerate the adoption of nanotechnology in various industries, such as medical, energy, electronics, transportation and materials, by providing relevant information, resources and tools, by connecting researchers and organizations, and by fostering knowledge sharing and cooperation.

For more information about the NWA, please visit http://www.nanotechnologyworld.org
Contact:
Marine Le Bouar
CEO marine@nanotechnologyworld.org
+65 3138 4138

NANOSCALE MATERIAL PATTERNING USING ATOMIC FORCE MICROSCOPY NANO-LITHOGRAPHY

John Paul Pineda, Charles Kim, Cathy Lee, Byong Kim, and Keibock Lee,
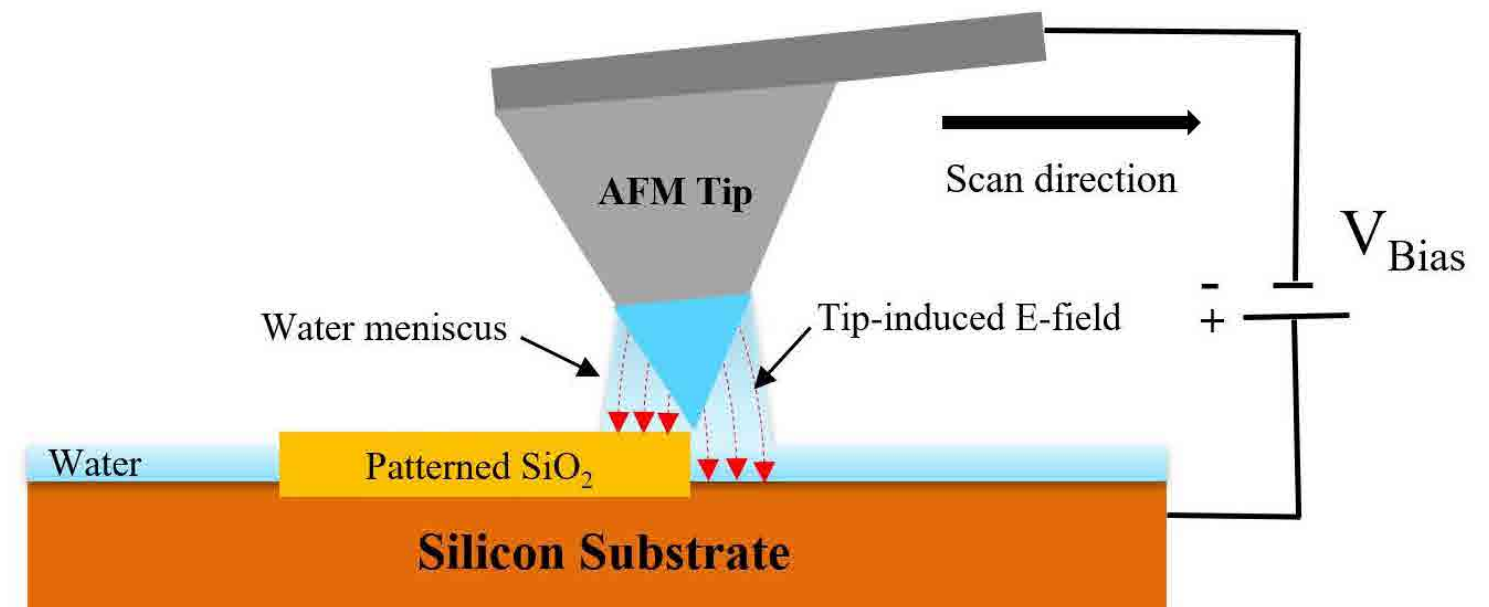Park Systems Inc., Santa Clara, CA USA

Figure 1. Schematic illustration of Bias-Assisted AFM Nanolithography [4, 5].

Introduction

Nanotechnology has received increased attention within the scientific community due to its application in a number of fields, ranging from electronics to biomedical technologies [1]. Progress in many of these applications depends mainly on the capability to fabricate nanostructured materials that include polymers and semiconductors, among others [2, 3]. Several methods have been introduced for the fabrication of nanostructures; the more common ones are electron beam lithography and focused ion beam lithography. However, these methods are not straightforward and are expensive to operate. One powerful method designed to overcome these problems is atomic force microscopy (AFM) nanolithography [1-3]. This technique is simple and less expensive [2]. AFM nanolithography is divided into two general groups based on their mechanistic and operational principles, bias-assisted and force-assisted AFM lithography [2]. In the bias-assisted method, a bias voltage is applied to the

tip to generate an oxide pattern on a metallic or semiconductor substrate [4, 5]. Whereas, the force-assisted method applies a large force to the tip to produce fine grooves on the surface of polymer-like samples by mechanically scratching, pushing or pulling the surface atoms and molecules with a sharp tip; the interaction between the tip and the sample is mainly mechanical [2, 3].

In this technical note, we demonstrate the capability of AFM nanolithography to generate nanopatterns by utilizing a Park NX10 Atomic Force Microscope. The tip bias mode is used to create oxide patterns on a silicon substrate. Successful pattern fabrication is confirmed by Lateral Force Microscopy (LFM). The integration of lithography and LFM mode with AFM enables it to fabricate nanopatterns and simultaneously acquire both topography and frictional data. The results obtained in this experiment confirms the fabricated oxide nanopatterns are successfully executed.

Experimental

A Park NX10 AFM was used for AFM nanolithography to draw nanopatterns onto a silicon substrate. LFM imaging was conducted after the lithography process to confirm the successful fabrication of the oxide patterns on the surface as well as to distinguish the surface difference between the oxide layers and silicon substrate. A PPP-CONTSCPt cantilever with a nominal spring constant (k = 0.2 N/m) and resonance frequency (f = 25 kHz) was utilized in the experiment.

Results and Discussion

Bias-Assisted AFM Nanolithography

Bias-Assisted AFM Nanolithography is a technique described as material modification (oxidation) through the application of voltage bias to the AFM tip. The applied bias on the tip results in the generation of an electric field between the tip and the sample. The field ionizes water molecules formed between the

tip and the sample, which leads to local anodic oxidation (LAO), used to fabricate nanoscale oxide features on the surface. In the lithography process, the tip acts as a nanoscale electrode for current injection or collection [1, 2]. The amount of oxide layer formed on the surface depends on the magnitude of the applied bias and humidity. A previous study [2] reported that the thickness of a pre-designed nanoscale oxide pattern of a device structure increased due to the increment of applied tip voltages. Therefore, it concluded the tip voltage influenced the amount of oxide formed in the surface. Figure 1 shows a schematic illustration of bias-assisted AFM nanolithography. In this study, Park lithography software was used to design and apply nanolithography to the sample surface. A silicon substrate was used as the sample. The application of -10 V resulted in a high electric field around the tip which led to the cleavage of water molecules into ions H+, OH- and O- ions [5]. The OH- and O- ions are then pushed away from the biased tip and react with silicon to form SiO_2. The nanoscale oxide pattern forms on the surface of the silicon substrate along the scan area of the lithography scan.

Lateral Force Microscopy

In Lateral Force Microscopy (LFM) mode, the vertical deflection and the torsion of the cantilever are measured and utilized to acquire topography and surface frictional characteristics of the sample. The cantilever movement in both the vertical direction and the torsion is tracked via a position sensitive photo detector (PSPD) that consists of four domains (a quad-cell), shown in Figure 2.
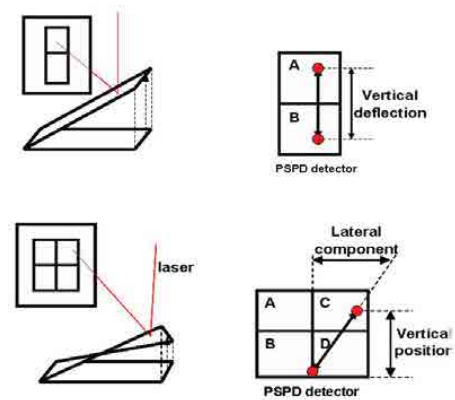
Figure 2. Schematic illustration of laser position on PSPD in the operation of AFM (top) and LFM (bottom).

Surface topographical information and frictional information are obtained using Equation 1 and 2.

Equation 1: Topographic information = (A+C) - (B+D)

Equation 2: Frictional information = (A+B) - (C+D)

Figure 3 shows the topography, frictional data and equivalent line profile of the images after the lithography process. The images were taken using LFM mode. Since LFM is a contact mode, both topography and frictional data can be acquired simultaneously, allowing for correlation between topographic and frictional properties. The AFM topography image (Figure 3b) reveals that the design is a Christmas ball pattern with a diameter of approximately 17 μm and composed of multiple tiny structures with

heights ranging from 0.2–1.5 nm. Figure 3e represents the line profiles that were generated using the Park XEI software to provide a more direct signal comparison. By analyzing the line profiles obtained from the LFM forward (green line) and backward (blue line) scans, we gain insight into the frictional characteristics of the sample. In the forward scan, the LFM signal shifted upward, indicating that the movement of the cantilever was hindered due to change in frictional force as the tip bypassed the oxide layer. Conversely, the LFM signal shifted downward during the backward scan, which, again, was a result of the cantilever being dragged by the surface because of the larger frictional interaction between the cantilever and the surface. As a result, we can conclude that the frictional coefficient of the oxide layer is higher than that of the silicon substrate.
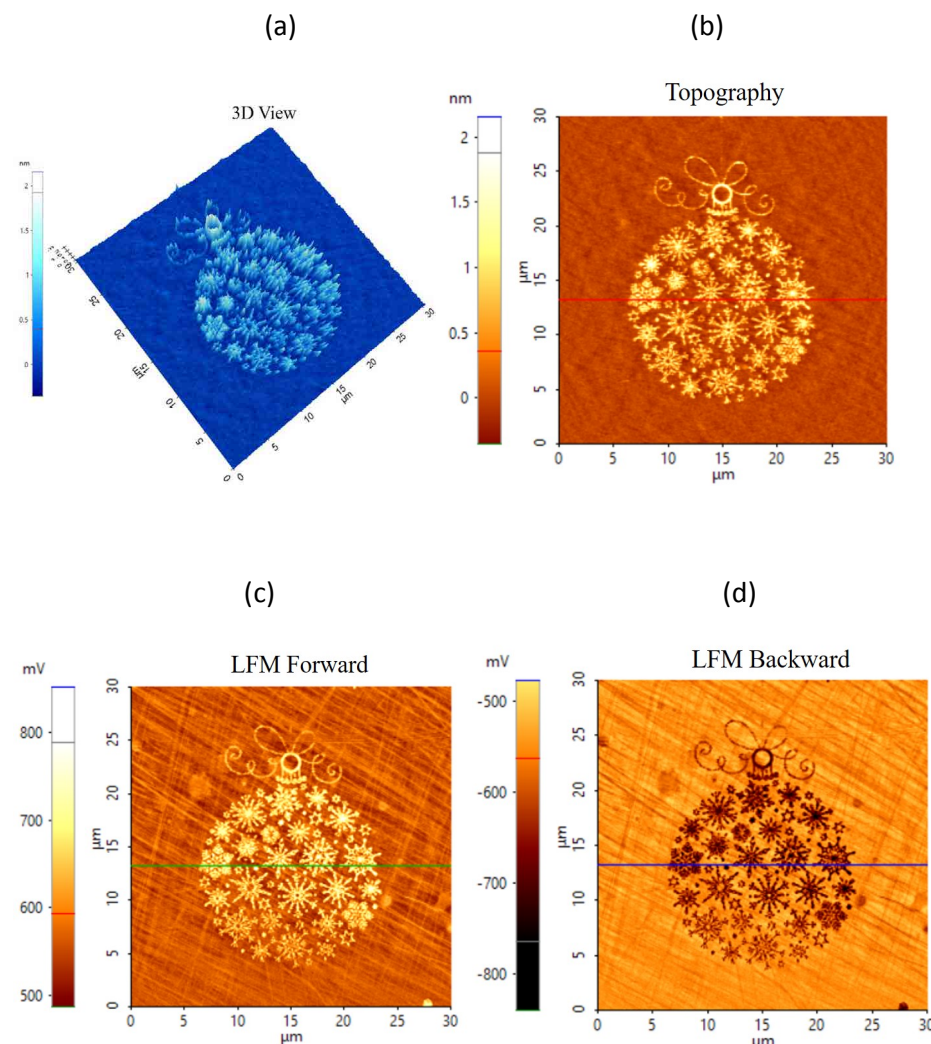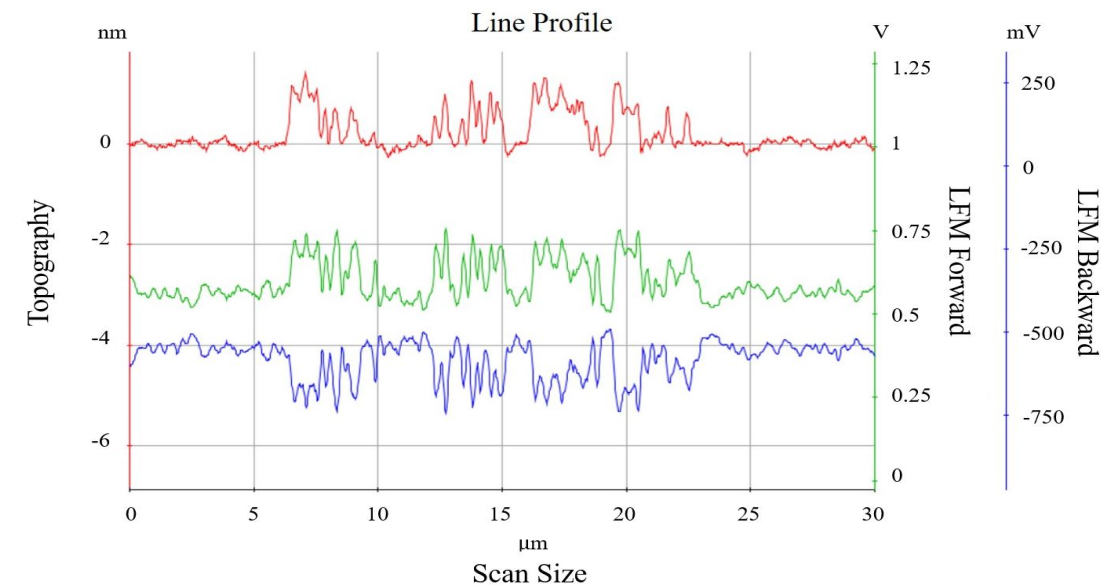
(a) (b)

(c) (d)

Figure 3. (a) 3D View, (b) Topography image, (c) LFM forward scan, (d) LFM backward scan.

(e) *Figure 3. (e) Line profiles plotted along red line seen in 3b, green line seen in 3c, and blue line seen in 3d.*

Conclusion

Here we have demonstrated the use of AFM nanolithography to generate nanoscale oxide patterns in a silicon substrate using a Park NX10 system. Voltage bias-mode technique was used in the AFM nanolithography process. The application of -10 V voltage bias on the tip led to successful fabrication of the nanoscale oxide features in the surface. LFM mode was also conducted and the results confirmed the successful fabrication of the oxide patterns. Overall, the

AFM nanolithography described in this study is an effective method to fabricate next generation materials and devices with nanoscale features.

References

1. A. Pimpin, et al., Review on Micro- and Nanolithography Techniques and their Applications. Engineering Journal.
2. S. Hutagalung, et al., Nanoscale Patterning by AFM Lithography and its Application on the Fabrication of Silicon Nanowire Devices. Sains Malaysiana 43(2), (2014): 267–272.
3. R. Garcia, et al., Advanced scanning probe lithography. Nature Nanotechnology 9, 577–587 (2014); doi:10.1038/nnano.2014.157
4. J. Voves, Nanoelectronics and nanolithography. https://www.researchgate.net/publication/228859246_Nanoelectronics_and_nanolithography
5. A. Bernal et al., LOCAL ANODIC OXIDATION ON SILICON (100) SUBSTRATES USING ATOMIC FORCE MICROSCOPY. http://www.scielo.org.co/pdf/dyna/v79n174/v79n174a08.pdf

BULK PHOTOVOLTAIC EFFECT IN FERROELECTRIC MATERIALS

DR. AKASH BHATNAGAR
AG LIGHT FOR HIGH-VOLTAGE PHOTOVOLTAICS

Zentrum für Innovationskompetenz, Martin Luther Universität Halle-Wittenberg, 06120 Halle (Saale), Germany

Dr. Akash Bhatnagar
Junior Research Group Leader
Light for High Voltage Photovoltaics,
The Centre for Innovation Competence
SiLi-nano®, Halle, Germany

The ever-growing demand for renewable energy cannot be overstated. Photovoltaic effect, which involves conversion of light to electricity has been considered as one of the most promising pathways. The field of photovoltaics is largely dominated with the use of semiconductor-based devices. The photovoltaic device primarily consists of a pn-junction with a space charge region at the interface between p- and n-type material [1]. The maximum efficiency obtainable from the pn-junction devices is defined by the Shockley-Quisser limit and has been calculated to be around 30% [2]. The innate limitation of the photovoltaic energy conversion in semiconductors has triggered the pursuit to find new materials that have a fundamentally different mechanism for charge separation.
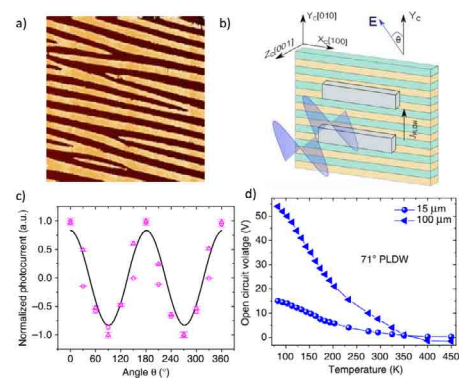

Figure 1. (a) Piezo force microscope 3.5 x 3.5 μm2 image acquired with Park XE-100. The brown and yellow colors show different ferroelectric domains. (b) Measurement geometry for BPV effect. (c) Angular dependent photovoltaic current. (d) Enhancement in Voc as the temperature is reduced in the case of 71° domains measured across 15 and 100 μm gaps [Taken from 4].

In this context, the photovoltaic effect in ferroelectric materials, i.e. bulk photovoltaic effect (BPV), has attracted a lot of attention. Ferroelectric materials can exist in different states of polarizations, or domains (Figure 1a), and can be switched from one state to the other by the application of electric field. The region in between the two domains is referred to as the domain wall. The photovoltaic effect in these materials is driven by the symmetry of the material rather a junction. As a result, the photocurrent generated is determined by a tensor which is largely analogous to the piezoelectric tensor of the material [3]. The photocurrent when measured with a linearly polarized light (Figure 1b), exhibits a dependency on the angle which the electric field of linearly polarized light makes with the direction of current flow (Figure 1c). Interestingly, the resultant open circuit voltages (Voc) are much higher than the band gap of the material and are in the range of 10–20V! Even higher voltages can be achieved if the overall conductivity of the samples is suppressed by lowering the temperature (Figure 1d) [4].

Another interesting aspect is the switch-ability of the effect. Unlike semiconductor-based photoeffect, the direction of photocurrent can be effectively reversed and under certain conditions the magnitude can be massively reduced (Figure 2). Such tunability arises from the ordering of domains which can manipulated by the application of electric field. Conversely, the BPV effect can be also utilized to determine the ordering of domains and estimate the net polarization.

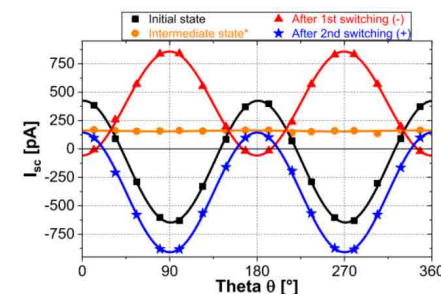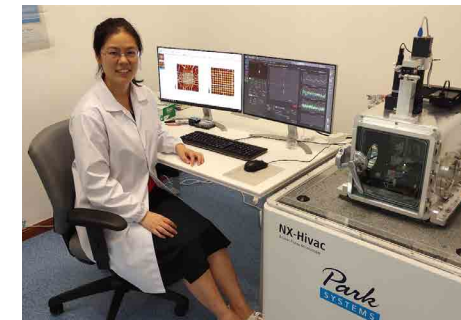However, there are some severe drawbacks that need to be addressed to

Figure 2. Photovoltaic current measured after each step of domain rearrangement upon application of switching field [Taken from 5].

widen the applicability of BPV effect. For instance, the band gap of ferroelectric material is typically above 2.8 eV, due to which only a small fraction of solar spectra can be utilized. Also, the current densities reported until now are way too low for any meaningful application. Nevertheless, with rapid development in thin film deposition and computational techniques, new material systems can be proposed and realized which would be able to overcome such limitations.

References:
1) Sze, S.M. (1981) Physics of semiconductor devices, John Wiley & Sons, INC
2) Shockley, W., and Queisser, H.J. (1961) Detailed balance limit of efficiency of p-n junction solar cells. J. Appl. Phys., 32 (3), 510–519.
3) Belinicher, V.I., Malinovskii, V.K., and Sturman, B.I. (1977). Photogalvanic effect in a crystal with polar axis. Soviet Physics – JETP 46 (2): 362–366
4) Bhatnagar, A., Roy Chaudhuri, A., Heon Kim, Y. et al. (2013). Role of domain walls in the abnormal photovoltaic effect in BiFeO3. Nature Communications 4 (May): 2835.
5) Knoche, D.S., Yun, Y., Ramakrishnegowda, N. et al. Domain and Switching Control of the Bulk Photovoltaic Effect in Epitaxial BiFeO3 Thin Films. Sci Rep 9, 13979 (2019)

FEI HUI, A POSTDOCTORAL FELLOW AT TECHNION-ISRAEL INSTITUTE OF TECHNOLOGY ANNOUNCED AS PARK AFM SCHOLAR

Abstract: Scanning probe microscopy for advanced nanoelectronics
As the size of electronic devices continues to shrink, characterization methods capable of precisely probing localized properties become increasingly important. Scanning probe microscopy techniques can examine local phenomena, and conductive atomic force microscopy can, in particular, study local electromechanical properties. Such techniques have already played a valuable role in the development of nanoelectronics, but their capabilities remain relatively limited compared with the probe stations typically used to examine electronic devices. Here, we discuss the potential of conductive atomic force microscopy in nanoelectronics. We explore possible characterization strategies, enhanced electronics for the technique and improved multiprobe approaches. We also propose a multiprobe scanning probe microscopy system that combines different types of probes and could allow multiple nanofabrication and characterization experiments to be carried out simultaneously under vacuum conditions.

Dr. Fei Hui at the AFM (Park NX-Hivac) lab
Fei Hui is currently a postdoctoral fellow at Technion-Israel Institute of Technology. She received her doctoral degree from the University of Barcelona in 2018. During her PhD, Dr. Hui was a visiting scholar at Massachusetts Institute of Technology (USA) for 12 months, where she learned chemical vapor deposition of two-dimensional (2D) materials (e.g. hexagonal boron nitride, graphene) on different substrates (i.e. Cu, Pt, Fe and Ni). She also received the Researcher Mobility Grant from the Royal Society of Chemistry, which supported her studies at the University of Cambridge (UK) for 6 months. In the Cambridge Graphene Center, she learned how to synthesize graphene oxide thin films and, more interestingly, how to cover nanoprobes with thin films of this material via spray technique. She has published over 40 research papers (11 papers are as first-author) in top journals including Nature Electronic, Advanced Functional Materials, ACS Applied Materials and Interfaces, and 2D Materials (among

others), and has more than 811 citations indicated by Google Scholar (https://scholar.google.com/. She has applied for two international patents, and one of them (cost-effective fabrication of ultra-durable graphene coated nanoprobes) attracted aroundapproximately $1 million investmentworth of investments.

Please summarize the research you do and explain why it is significant?
My research topic is the development of two-dimensional (2D) materials based electronic devices. We are aiming to integrate 2D materials (e.g. hexagonal boron nitride, graphene or molybdenum disulfide) into electronic devices (e.g. memristors or field effect transistors). Due to the atomic thin layer and extraordinary properties (e.g. high thermal and electrical conductivity, flexibility and transparency) of 2D materials, it allows us to design miniaturized devices, which exhibit some exotic performances that conventional transition metal oxides (e.g. HfO2)-based devices do not show. More specifically, I first synthesized monolayer or multilayer 2D materials using chemical vapor deposition (CVD) methodology. After growth I used several techniques to analyze the quality of these materials, mainly Raman Spectroscopy and cross-sectional transmission electron microscopy (X-TEM), but the technique that provided me best results was conductive atomic force microscopy (CAFM). Using this technique, I explored the dielectric properties of hexagonal boron nitride (h-BN) and graphene oxide (GO), including tunneling current, charge trapping, trap-assisted tunneling, stress-induced leakage current, dielectric breakdown and resistive switching (RS). I also used these 2D materials to fabricate memristive devices, and analyzed them using a probe station connected to a semiconductor parameter analyzer (working in different atmospheres).

How might your research be used?
In my work, I employed a scalable CVD technique to synthesis large sizes of 2D materials, which allow us to fabricate high-yield electronic devices and study their device-to-device variability. Moreover, this methodology is more compatible with

and useful for the industry than single/few devices fabricated by mechanical exfoliation. In our previous work, we have proved that h-BN can be used as a RS medium and the metal/h-BN/metal devices showed both volatile and non-volatile RS behaviors, enabling the emulation of a range of synaptic-like behavior, including both short- and long- term plasticity. Therefore, our research would accelerate the use of 2D materials for building future wafer-scale and high-density electronic memories and/or artificial neural networks.

What features of Park AFM are the most beneficial and why?
The Park AFM system is a powerful tool that provides us with more accurate and reliable information under different conditions (ambient and vacuum conditions), which is extremely important for the research field of nanoscience. First of all, the true non-contact mode allows us to acquire the topographic information, such as the wrinkles of 2D materials or some tiny particles, without the damage of probes and surface modification of specimens. Second, the image/position drift is negligible, we can perform spectroscopy measurements (e.g. current vs. voltage, force vs. distance) at specific locations or in a matrix pattern and then go back to them exactly. Moreover, the navigation and the software interface are quite user-friendly, which save us much more time.

Why is the Park AFM important for your research?
This Park NX-Hivac system is able to simultaneously perform four tasks that are essential to study RS reliably:This Park NX-Hivac system is able to simultaneously perform four tasks that are essential to study RS reliably: i) measure currents in tapping mode (to avoid premature tip wearing and material damage); ii) measure high currents from picoamperes to milliamperes in both polarities by using a logarithmic preamplifier (to monitor the set/reset transitions in situ); iii) measure in high vacuum up to 10-6 torr (to avoid local anodic oxidation and unwanted moisture-related reactions); and, iv) measure at high temperatures up to 600 ºC (not only to study reliability, but also to evaporate all water molecules on the materials after pumping the vacuum). The need of these four features to reliably measure RS at the nanoscale is extensively described in the book (*Conductive Atomic Force Microscopy: Applications in Nanomaterials,* ISBN: 978-3-527-69978-0, Wiley-VCH Weinheim, Germany, 2017) *edited by Prof. Mario Lanza, who is a leading expert in CAFM science, and there is no other equipment in the world that can carry out all these actions.simultaneously. The use of this tool will be a high advantage compared to other groups.*
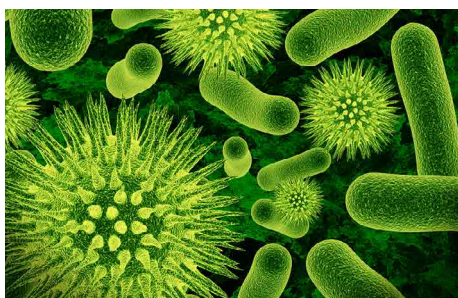
NEW SURFACTANT DESIGN

MATERIALS MATTER

Column Highlighting Topics Presented in Dr. Advincula's Monthly Webinars on Advancements in Material Science

Dr. Rigoberto Advincula, Professor, Macromolecular Science & Engineering, Case Western Reserve University

Microbial Biosurfactants Market

Photo Caption: The global market for Microbial Biosurfactants is expected to show a healthy CAGR of +4% over the course of the given forecast period of 2019 to 2026.

What is surfactant chemistry?

Surface science based on surfactant chemistry includes common surfactant hydrophones and hygrophilous and different unconventional surfactant designs, polymeric surfactants, bio-derived surfactants, linear and nonlinear surfactants which have applications in consumer products, oil and gas, chemistry, paints and coatings, and more. Newer surfactant designs include bio surfactants derived from a natural source and in terms of sustainability are typically non toxic and therefore preferred in some applications.

What is the importance of surfactants?

Surfactants are essential for life because this is what constitutes your cell membrane. This is what constitutes the surfactants in your lungs that allow you to breathe normally. And surfactants are found in many applications from detergents, cosmetics, pharmaceutical, textile, fiber, plastic composites, and metal processing which almost makes them ubiquitous that we don't pay attention to what they do because they simply work,

but sometimes they can be a problem. For example, when we talk about detergency, we are concerned with the critical amounts of concentration and stability in different pH, salt conditions and bio-degradability.

A universal surfactant has many uses, especially if they can be derived from sources such as oleic acids or fatty acids, a basic surfactant design, surfactant is a word that is derived from "surface active agent". The building block is the hydrophobic part typically is an upward chain and a hydrophilic part, which can be anionic, cationic, zwitterionic or even non ionic. So the balance of this two parts makes for what we call an amphiphile or amphiphilic.

What are the categories of surfactants?

The hydrophilic group of surfactants are water loving or water-soluble and the hydrophobic group or hydrophobe is water hating or lipophilic (oil loving). So the composition of these two or the balance of these two makes up for your surfactant. Now typically a surfactant can be classified based on the head group. It can be anionic, so the most common wants are based on sodium dodecyl sulfate, or SDS. Cationic, it can be cetrimonium bromide or CTAB. Zwitterion will be based on the betaine or sultriness and of course lipids are zwitterion. And the nonionic are essentially neutral and a lot of them are polymer base such as the polyethylene glycol alkyl ethers.

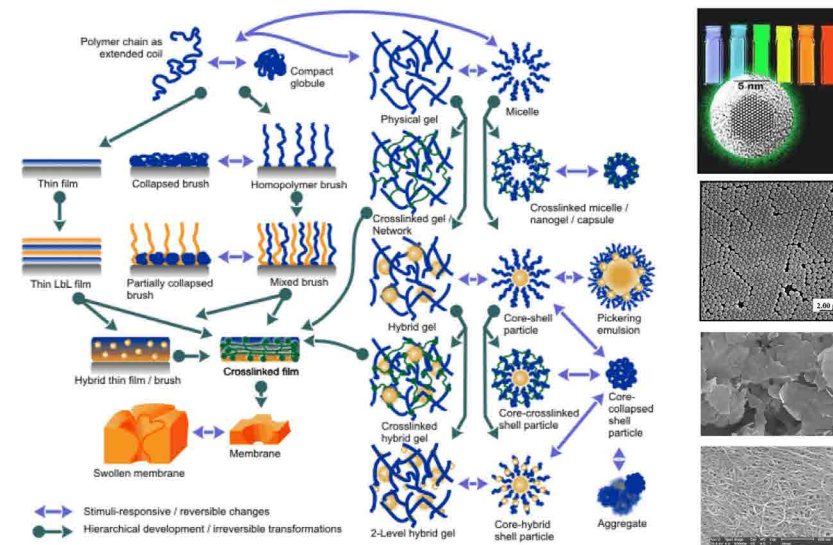### What is the importance of the critical micelle concentration (CMC)?

The micelle basically is an aggregate, a dynamic aggregate of surfactants that are stabilized in solution versus that of

surfactants at the air water interface and you need a minimum amount of micelle to form this surfactant to form of this micelle to achieve micellization and this can be done by measuring properties such as the surface tension, ionic conductivity or size directly from lights. A micelle can be extended to be spherical to worm like micelles to vesicles, bilayers. Essentially, these are what we call liquid crystalline mesophases or even lyotropic phases. That is a result of increasing concentration or the change in the geometry of the surfactant based on what they called the packing parameter. The critical packing parameter is characterized by the volume of the hydrophobic part, the optimal surface area occupied by the head group and the critical land of the hydrophobic tail. You can use TEM, transmission electro microscopy to directly observe these vesicles or micelles effectively.

What is a typical surfactant design?

Typical head groups or hydrophilic part could be anionic and most common will be the carboxyl. Cationic, a lot of them are based on quaternary ammonium halides and sometimes amoeba selenium derivatives. A lot of them are water soluble polymers such as polyethylene glycol. A typical hydrophobe will be a straight-chain alkyl group. It can be anywhere from C eight to C 22 it can be a branch chain alkyl group to internal substitution. It can be an unsaturated alkyl chemical chain, meaning it has a double bond such as those derived from a vegetable oil, or it can be an alkylbenzene with various substitutions and pattern. And of course other variations can include siloxane or fluorinated or per fluorinated-alkyl chains.

Polymers at Interfaces, Colloidal Phenomena, Nanomaterials

- ➤ Stimuli-responsive / reversible changes
- ➤ Hierarchical development / irreversible transformations

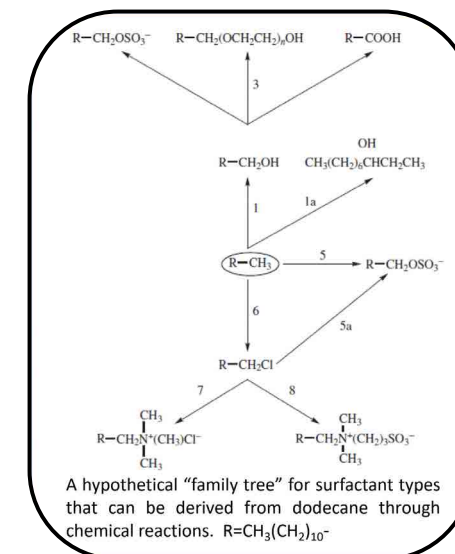A surfactant family tree essentially allows you to take an alkyl chain.

A polymer or macromolecule is accurately a nanomaterial, a nanomaterial that has surfactant capabilities that is able to order cell assemble on surfaces, flat surfaces, modification in layers, eventually macroscopic properties or the application of polymers towards gelation, emulsion, different types of cross linking and hydro gel type of systems. These are based on co-polymer type of arrangements. A predominant type of a co-polymer that is used as a surfactant RD block, co-polymer linear systems and block copolymers are found in additives, elastomers, they have interesting mesophases in which you can order the chain length and the molecular way to produce different phases such as cylindrical, lamellar spherical and so on.

What are bio surfactants?

Bio surfactant means it's a surfactant derived from a natural source. Typically this comes from plants, animals or extraction from microbial cells and the separation procedures simply involves extraction, precipitation and distillation. And a lot of them of course appeal in terms of sustainability or use of natural derived surfactants versus that of synthetic and Petro based surfactants. They are typically non toxic and therefore are preferred in some applications.

A polymer surfactant is derived from a macromolecule. A bio surfactant can be

Basic surfactant building blocks - surfactant family tree

A hypothetical "family tree" for surfactant types that can be derived from dodecane through chemical reactions. $R=CH_3(CH_2)_{10}$-

When talking about the root of surfactant family tree, n-dodecane was considered

1-dodecanol or 3-dodecanol are still low solubility in water

Sodium dodecylsulfate (SDS) are the most extensively studied and best understood surfactant

Dodecyltrimethylammonium chloride is a water-soluble compound exhibiting some surfactant properties.
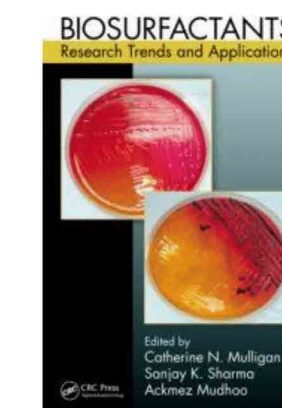
A difunctional material such as N, N-dimethyl-3-aminopropane-1-sulfonic acid is type of zwitterionic or amphoteric surfactants.

derived from a microorganisms or bio base feed stacks, a nonlinear surfactant or an unconventional nanoparticle surfactant and their applications in viscoelastics surfactants.

Bio surfactants can be derived by extraction directly from plants and animals. However, certain enzymes or microbes are coded to produce different surfactants. This can be based on genetic engineering and harvested as well in a bioreactor. So for example some of these bio-based surfactants can be programmed to have the presence of carbon, nitrogen or even multi valent ions. So in a micro organism for example, it will produce the surfactants and can be harvested separately from the micro organisms. A bio-reactor requires media, fermentation, and a procedure and product recovery.

Bio surfactants are used in a number of applications such as heavy metal remediation or they can be derived to become potent antibiotics, especially the quaternary amine containing derivatives. And they can be used also for different types of agriculture. For example, a bio surfactant can be used to remove styrene from contaminated soil. Styrene is a monomer, used to make polystyrene or petroleum based polymer and this is a demonstration that it can be used for remediation or bio-remediation to remove a styrene or even other PCB back off contaminants.

For the complete webinar on Surfactant Design and other webinars with Dr. Advincula: https://www.parksystems.com/medias/nano-academy/webinars/115-webinars/1674-new-surfactant-design

BIOSURFACTANTS
Research Trends and Applications

Edited by
Catherine N. Mulligan
Sanjay K. Sharma
Ackmez Mudhoo

Park NX12
The most versatile
atomic force microscope
for analytical chemistry

- *Built on proven Park AFM performance*
- *Equipped with inverted optical microscope*

Proven Performance
The Park NX12 is based on the Park NX10, one of the most trusted and widely used AFMs for research. Users can rest assured that they are taking measurements with a cutting-edge tool.

Built for Versatility
Multi-user labs need a versatile microscope to meet a wide range of needs. The Park NX12 was built from the ground up to be a flexible modular platform to allow shared facilities to invest in a single AFM to perform any task.

Competitive Pricing
Early career researchers need to do great work with cost-effective tools. Despite its outstanding pedigree, the Park NX12 is priced affordably—ideal for those on a constrained budget.

To learn more about Park NX12
Please visit parksystems.com/nx12 or email: inquiry@parksystems.com

Park
SYSTEMS
parksystems.com